

A Generalized Algorithm for the Generation of Correlated Rayleigh Fading Envelopes in Wireless Channels

Le Chung Tran

Telecommunications and Information Technology Research Institute (TITR), School of Electrical, Computer and Telecommunications Engineering, University of Wollongong, Wollongong NSW 2522, Australia
Email: lct71@uow.edu.au

Tadeusz A. Wysocki

School of Electrical Computer and Telecommunications Engineering, Faculty of Informatics, University of Wollongong, Wollongong NSW 2522, Australia
Email: wysocki@uow.edu.au

Alfred Mertins

Signal Processing Group, Department of Physics, University of Oldenburg, 26111 Oldenburg, Germany
Email: alfred.mertins@uni-oldenburg.de

Jennifer Seberry

School of Information Technology and Computer Science, Faculty of Informatics, University of Wollongong, Wollongong NSW 2522, Australia
Email: jennie@uow.edu.au

Received 23 January 2005; Revised 6 July 2005; Recommended for Publication by Wei Li

Although generation of correlated Rayleigh fading envelopes has been intensively considered in the literature, all conventional methods have their own shortcomings, which seriously impede their applicability. A very general, straightforward algorithm for the generation of an *arbitrary* number of Rayleigh envelopes with *any desired, equal or unequal* power, in wireless channels either *with* or *without* Doppler frequency shifts, is proposed. The proposed algorithm can be applied to the case of *spatial correlation*, such as with multiple antennas in multiple-input multiple-output (MIMO) systems, or *spectral correlation* between the random processes like in orthogonal frequency-division multiplexing (OFDM) systems. It can also be used for generating correlated Rayleigh fading envelopes in either *discrete-time instants* or a *real-time scenario*. Besides being *more generalized*, our proposed algorithm is *more precise*, while overcoming all shortcomings of the conventional methods.

Keywords and phrases: correlated Rayleigh fading envelopes, antenna arrays, OFDM, MIMO, Doppler frequency shift.

1. INTRODUCTION

In orthogonal frequency-division multiplexing (OFDM) systems, the fading affecting carriers may have cross-correlation due to the small coherence bandwidth of the channel, or due to the inadequate frequency separation between the carriers. In addition, in multiple-input multiple-output (MIMO) systems where multiple antennas are used to transmit and/or

receive signals, the fading affecting these antennas may also experience cross-correlation due to the inadequate separation between the antennas. Therefore, a generalized, straightforward and, certainly, correct algorithm to generate correlated Rayleigh fading envelopes is required for the researchers wishing to analyze theoretically and simulate the performance of systems.

Because of that, generation of correlated Rayleigh fading envelopes has been intensively mentioned in the literature, such as [1, 2, 3, 4, 5, 6, 7, 8, 9, 10, 11, 12, 13]. However, besides not being adequately generalized to be able to apply to various scenarios, all conventional methods have their own

This is an open access article distributed under the Creative Commons Attribution License, which permits unrestricted use, distribution, and reproduction in any medium, provided the original work is properly cited.

shortcomings which seriously limit their applicability or even cause failures in generating the desired Rayleigh fading envelopes.

In this paper, we modify existing methods and propose a generalized algorithm for generating correlated Rayleigh fading envelopes. Our modifications are *simple*, but *important* and also very *efficient*. The proposed algorithm thus incorporates the advantages of the existing methods, while overcoming all of their shortcomings. Furthermore, besides being *more generalized*, the proposed algorithm is *more accurate*, while providing *more useful features* than the conventional methods.

The paper is organized as follows. In Section 2, a summary of the shortcomings of conventional methods for generating correlated Rayleigh fading envelopes is derived. In Sections 3.1 and 3.2, we shortly review the discussions on the correlation property between the transmitted signals as functions of time delay and frequency separation, such as in OFDM systems, and as functions of spatial separation between transmission antennas, such as in MIMO systems, respectively. In Section 4, we propose a very general, straightforward algorithm to generate correlated Rayleigh fading envelopes. Section 5 derives an algorithm to generate correlated Rayleigh fading envelopes in a real-time scenario. Simulation results are presented in Section 6. The paper is concluded by Section 7.

2. SHORTCOMINGS OF CONVENTIONAL METHODS AND AIMS OF THE PROPOSED ALGORITHM

We first analyze the shortcomings of some conventional methods for the generation of correlated Rayleigh fading envelopes.

In [3], the authors derived fading correlation properties in antenna arrays and, then, briefly mentioned the algorithm to generate complex Gaussian random variables (with Rayleigh envelopes) corresponding to a desired correlation coefficient matrix. This algorithm was proposed for generating *equal power* Rayleigh envelopes only, rather than *arbitrary (equal or unequal) power* Rayleigh envelopes.

In [4, 5], the authors proposed different methods for generating only $N = 2$ *equal power* correlated Rayleigh envelopes. In [6], the authors generalized the method of [5] for $N \geq 2$. However, in this method, Cholesky decomposition [7] is used, and consequently, the covariance matrix must be positive definite, which is not always realistic. An example, where the covariance matrix is *not* positive definite, is derived later in Example 1 of Section 4.1 of this paper.

These methods were then more generalized in [8], where one can generate *any number* of Rayleigh envelopes corresponding to a desired covariance matrix and with *any power*, that is, even with *unequal power*. However, again, the covariance matrix *must be positive definite* in order for Cholesky decomposition to be performable. In addition, the authors in [8] forced the covariances of the complex Gaussian random variables (with Rayleigh fading envelopes) to be *real* (see [8, (8)]). This limitation *prohibits* the use of their method in

various cases because, in fact, the covariances of the complex Gaussian random variables are more likely to be complex.

In [2], the authors proposed a method for generating *any number* of Rayleigh envelopes with *equal power* only. Although the method of [2] works well in various cases, it *fails* to perform Cholesky decomposition for some complex covariance matrices in Matlab due to the roundoff errors of Matlab.¹ This shortcoming is overcome by some modifications mentioned later in our proposed algorithm.

More importantly, the method proposed in [2] *fails* to generate Rayleigh fading envelopes corresponding to a desired covariance matrix in a real-time scenario *where Doppler frequency shifts are considered*. This is because passing Gaussian random variables with variances assumed to be equal to one (for simplicity of explanation) through a Doppler filter changes remarkably the variances of those variables. The variances of the variables at the outputs of Doppler filters are *not* equal to one any more, but depend on the variance of the variables at the inputs of the filters as well as the characteristics of those filters. The authors in [2] did not realize this variance-changing effect caused by Doppler filters. We will return to this issue later in this paper.

For the aforementioned reasons, a *more generalized* algorithm is required to generate *any number* of Rayleigh fading envelopes with *any power (equal or unequal power)* corresponding to *any desired* covariance matrix. The algorithm should be applicable to both *discrete time instant* scenario and *real-time* scenario. The algorithm is also expected to overcome roundoff errors which may cause the interruption of Matlab programs. In addition, the algorithm should work well, regardless of the positive definiteness of the covariance matrices. Furthermore, the algorithm should provide a straightforward method for the generation of complex Gaussian random variables (with Rayleigh envelopes) with correlation properties as functions of *time delay* and *frequency separation* (such as in OFDM systems), or *spatial separation* between transmission antennas (like with multiple antennas in MIMO systems). This paper proposes such an algorithm.

3. BRIEF REVIEW OF STUDIES ON FADING CORRELATION CHARACTERISTICS

In this section, we shortly review the discussions on the correlation property between the transmitted signals as func-

¹It has been well known that Cholesky decomposition may not work for the matrix having eigenvalues being equal or close to zeros. We consider the following covariance matrix \mathcal{K} , for instance:

$$\mathcal{K} = \begin{bmatrix} 1.04361 & 0.7596 - 0.3840i & 0.6082 - 0.4427i & 0.4085 - 0.8547i \\ 0.7596 + 0.3840i & 1.04361 & 0.7780 - 0.3654i & 0.6082 - 0.4427i \\ 0.6082 + 0.4427i & 0.7780 + 0.3654i & 1.04361 & 0.7596 - 0.3840i \\ 0.4085 + 0.8547i & 0.6082 + 0.4427i & 0.7596 + 0.3840i & 1.04361 \end{bmatrix}$$

Cholesky decomposition does not work for this covariance matrix although it is positive definite.

tions of time delay and frequency separation, such as in OFDM systems, and as functions of spatial separation between transmission antennas, such as in MIMO systems. These discussions were originally derived in [3, 9], respectively.

This review aims at facilitating readers to apply our proposed algorithm in different scenarios (i.e., *spectral correlation*, such as in OFDM systems, or *spatial correlation*, such as in MIMO systems) as well as pointing out the condition for the analyses in [3, 9] to be applicable to our proposed algorithm (i.e., these analyses are applicable to our algorithm if the powers (variances) of different random processes are assumed to be the same).

3.1. Fading correlation as functions of time delay and frequency separation

In [9], Jakes considered the scenario where all complex Gaussian random processes with Rayleigh envelopes have equal powers σ^2 and derived the correlation properties between random processes as functions of both time delay and frequency separation, such as in OFDM systems. Let $z_k(t)$ and $z_j(t)$ be the two zero-mean complex Gaussian random processes at time instant t , corresponding to frequencies f_k and f_j , respectively. Denote

$$\begin{aligned} x_k &\triangleq \text{Re}(z_k(t)), & y_k &\triangleq \text{Im}(z_k(t)), \\ x_j &\triangleq \text{Re}(z_j(t + \tau_{k,j})), & y_j &\triangleq \text{Im}(z_j(t + \tau_{k,j})), \end{aligned} \quad (1)$$

where $\tau_{k,j}$ is the arrival time delay between two signals and $\text{Re}(\cdot)$, $\text{Im}(\cdot)$ are the real and imaginary parts of the argument, respectively. By definition, the covariances between the real and imaginary parts of $z_k(t)$ and $z_j(t + \tau_{k,j})$ are

$$\begin{aligned} R_{xxk,j} &\triangleq E(x_k x_j), & R_{yyk,j} &\triangleq E(y_k y_j), \\ R_{xyk,j} &\triangleq E(x_k y_j), & R_{yxk,j} &\triangleq E(y_k x_j). \end{aligned} \quad (2)$$

Then, those covariances have been derived in [9, (1.5-20)] as

$$\begin{aligned} R_{xxk,j} &= R_{yyk,j} = \frac{\sigma^2 J_0(2\pi F_m \tau_{k,j})}{2[1 + (\Delta\omega_{k,j} \sigma_\tau)^2]}, \\ R_{xyk,j} &= -R_{yxk,j} = -\Delta\omega_{k,j} \sigma_\tau R_{xxk,j}, \end{aligned} \quad (3)$$

where σ^2 is the variance (power) of the complex Gaussian random processes ($\sigma^2/2$ is the variance per dimension); J_0 is the first-kind Bessel function of the zeroth-order; F_m is the maximum Doppler frequency $F_m = v/\lambda = v f_c/c$. In this formula, λ is the wavelength of the carrier, f_c is the carrier frequency, c is the speed of light, and v is the mobile speed; $\Delta\omega_{k,j} = 2\pi(f_k - f_j)$ is the angular frequency separation between the two complex Gaussian processes with Rayleigh envelopes at frequencies f_k and f_j ; σ_τ is the root-mean-square (rms) delay spread of the wireless channel.

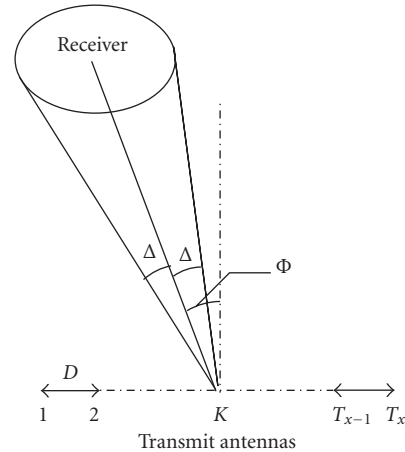


FIGURE 1: Model to examine the spatial correlation between transmitter antennas.

It should be emphasized that, the equalities (3) hold only when the set of *multipath channel coefficients*, which were denoted as C_{nm} and derived in [9, (1.5-1) and (1.5-2)], as well as the *powers* are assumed to be the *same* for different random processes (with different frequencies). Readers may refer to [9, pages 46–49] for an explicit exposition.

3.2. Fading correlation as functions of spatial separation in antenna arrays

The fading correlation properties between wireless channels as functions of antenna spacing in multiple antenna systems have been mentioned in [3]. Figure 1 presents a typical model of the channel where all signals from a receiver are assumed to arrive at T_x antennas within $\pm\Delta$ at angle Φ ($|\Phi| \leq \pi$). Let λ be the wavelength, D the distance between the two adjacent transmitter antennas, and $z = 2\pi(D/\lambda)$. In [3], it is assumed that fading corresponding to different receivers is independent. This is reasonable if receivers are not on top of each other within some wavelengths and they are surrounded by their own scatterers. Consequently, we only need to calculate the correlation properties for a typical receiver. The fading in the channel between a given k th transmitter antenna and the receiver may be considered as a zero-mean, complex Gaussian random variable, which is presented as $b^{(k)} = x^{(k)} + iy^{(k)}$. Denote the covariances between the real parts as well as the imaginary parts themselves of the fading corresponding to the k th and j th transmitter antennas² to be $R_{xxk,j}$ and $R_{yyk,j}$, while those terms between the real and imaginary parts of the fading to be $R_{xyk,j}$ and $R_{yxk,j}$. The terms $R_{xxk,j}$, $R_{yyk,j}$, $R_{xyk,j}$ and $R_{yxk,j}$ are similarly defined as (2). Then, it has been proved that the closed-form expressions of these covariances normalized by the variance per dimension (real and imaginary) are (see [3,

²Note that k and j here are antenna indices, while they are frequency indices in Section 3.1.

(A. 19) and (A. 20))]

$$\begin{aligned}\tilde{R}_{xxk,j} &= \tilde{R}_{yyk,j} \\ &= J_0(z(k-j)) + 2 \sum_{m=1}^{\infty} J_{2m}(z(k-j)) \cos(2m\Phi) \frac{\sin(2m\Delta)}{2m\Delta},\end{aligned}\quad (4)$$

$$\begin{aligned}\tilde{R}_{xyk,j} &= -\tilde{R}_{yxk,j} = 2 \sum_{m=0}^{\infty} \left[J_{2m+1}(z(k-j)) \sin[(2m+1)\Phi] \right. \\ &\quad \left. \times \frac{\sin[(2m+1)\Delta]}{(2m+1)\Delta} \right],\end{aligned}\quad (5)$$

where $\tilde{R}_{k,j} = 2R_{k,j}/\sigma^2$. In other words, we have

$$R_{k,j} = \frac{\sigma^2 \tilde{R}_{k,j}}{2}. \quad (6)$$

In these equations, J_q is the first-kind Bessel function of the integer order q , and $\sigma^2/2$ is the variance per dimension of the received signal at each transmitter antenna, that is, it is assumed in [3] that the signals corresponding to different transmitter antennas have *equal* variances σ^2 .

Similarly to Section 3.1, the equalities (4) and (5) hold only when the set of *multipath channel coefficients*, which were denoted as g_n and derived in [3, (A-1)], and the *powers* are assumed to be the *same* for different random processes. Readers may refer to [3, pages 1054–1056] for an explicit exposition.

4. GENERALIZED ALGORITHM TO GENERATE CORRELATED, FLAT RAYLEIGH FADING ENVELOPES

4.1. Covariance matrix of complex Gaussian random variables with Rayleigh fading envelopes

It is known that Rayleigh fading envelopes can be generated from zero-mean, complex Gaussian random variables. We consider here a column vector \mathbb{Z} of N zero-mean, *complex* Gaussian random variables with variances (or powers) $\sigma_{g_j}^2$, for $j = 1, \dots, N$. Denote $\mathbb{Z} = (z_1, \dots, z_N)^T$, where z_j ($j = 1, \dots, N$) is regarded as

$$z_j = r_j e^{i\theta_j} = x_j + iy_j. \quad (7)$$

The modulus of z_j is $r_j = \sqrt{x_j^2 + y_j^2}$. It is assumed that the phases θ_j 's are independent, identically uniformly distributed random variables. As a result, the real and imaginary parts of each z_j are independent (but z_j 's are not necessarily independent), that is, the covariances $E(x_j y_j) = 0$ for all j and therefore, r_j 's are *Rayleigh envelopes*.

Let $\sigma_{g_{xj}}^2$ and $\sigma_{g_{yj}}^2$ be the variances per dimension (real and imaginary), that is, $\sigma_{g_{xj}}^2 = E(x_j^2)$, $\sigma_{g_{yj}}^2 = E(y_j^2)$. Clearly, $\sigma_{g_j}^2 = \sigma_{g_{xj}}^2 +$

$\sigma_{g_{yj}}^2$. If $\sigma_{g_{xj}}^2 = \sigma_{g_{yj}}^2$, then $\sigma_{g_j}^2 = \sigma_{g_{xj}}^2 = \sigma_{g_{yj}}^2/2$. Note that we consider a very general scenario where the variances (powers) of the real parts are not necessarily equal to those of the imaginary parts. Also, the powers of Rayleigh envelopes denoted as $\sigma_{r_j}^2$ are not necessarily equal to one another. Therefore, the scenario where the variances of the Rayleigh envelopes are equal to one another and the powers of real parts are equal to those of imaginary parts, such as the scenario mentioned in either Section 3.1 or Section 3.2, is considered as a particular case.

For $k \neq j$, we define the covariances $R_{xxk,j}$, $R_{yyk,j}$, $R_{xyk,j}$, and $R_{yxk,j}$ between the real as well as imaginary parts of z_k and z_j , similarly to those mentioned in (2).

By definition, the covariance matrix \mathcal{K} of \mathbb{Z} is

$$\mathcal{K} = E(\mathbb{Z}\mathbb{Z}^H) \triangleq [\mu_{k,j}]_{N \times N}, \quad (8)$$

where $(\cdot)^H$ denotes the Hermitian transposition operation and

$$\mu_{k,j} = \begin{cases} \sigma_{g_j}^2 & \text{if } k \equiv j, \\ (R_{xxk,j} + R_{yyk,j}) - i(R_{xyk,j} - R_{yxk,j}) & \text{if } k \neq j. \end{cases} \quad (9)$$

In reality, the covariance matrix \mathcal{K} is *not* always positive semidefinite. An example where the covariance matrix \mathcal{K} is *not* positive semidefinite is derived as follows.

Example 1. We examine an antenna array comprising 3 transmitter antennas. Let D_{kj} , for $k, j = 1, \dots, 3$, be the distance between the k th antenna and the j th antenna. The distance D_{jk} between j th antenna and the k th antenna is then $D_{jk} = -D_{kj}$. Specifically, we consider the case

$$\begin{aligned}D_{21} &= 0.0385\lambda, \\ D_{31} &= 0.1789\lambda, \\ D_{32} &= 0.1560\lambda,\end{aligned}\quad (10)$$

where λ is the wavelength. Clearly, these antennas are *neither* equally spaced, *nor* positioned in a straight line. Instead, they are positioned at the 3 peaks of a triangle.

If the receiver antenna is far enough from the transmitter antennas, we can assume that all signals from the receiver arrive at the transmitter antennas within $\pm\Delta$ at angle Φ (see Figure 1 for the illustration of these notations). As a result, the analytical results mentioned in Section 3.2 with small modifications can still be applied to this case. In particular, covariance matrix \mathcal{K} can still be calculated following (4), (5), (6), (8), and (9), provided that, in (4) and (5), the products $z(k-j)$ (or $2\pi D(k-j)/\lambda$) are replaced by $2\pi D_{kj}/\lambda$. This is because, in our considered case, D_{kj} are the actual distances between the k th transmitter antenna and the j th transmitter antenna, for $k, j = 1, \dots, 3$.

Further, we assume that the variance σ^2 of the received signals at each transmitter antenna in (6) is unit, that is, $\sigma^2 = 1$. We also assume that $\Phi = 0.1114\pi$ rad and $\Delta = 0.1114\pi$ rad.

In order to examine the performance of the considered system, the Rayleigh fading envelopes are required to be simulated. In turn, the covariance matrix of the complex Gaussian random variables corresponding to these Rayleigh envelopes must be calculated. Based on the aforementioned assumptions, from the theoretically analytical equations (4), (5), and (6), and the definition equations (8) and (9), we have the following desired covariance matrix for the considered configuration of transmitter antennas:

$$\mathcal{K} = \begin{bmatrix} 1.0000 & 0.9957 + 0.0811i & 0.9090 + 0.3607i \\ 0.9957 - 0.0811i & 1.0000 & 0.9303 + 0.3180i \\ 0.9090 - 0.3607i & 0.9303 - 0.3180i & 1.0000 \end{bmatrix}. \quad (11)$$

Performing eigen decomposition, we have the following eigenvalues: -0.0092 ; 0.0360 ; and 2.9733 . Therefore, \mathcal{K} is *not* positive semidefinite. This also means that \mathcal{K} is *not* positive definite.

It is important to emphasize that, from the mathematical point of view, covariance matrices are *always* positive semidefinite by definition (8), that is, the eigenvalues of the covariance matrices are *either* zero *or* positive. However, this does not contradict the above example where the covariance matrix \mathcal{K} has a negative eigenvalue. The main reason why the desired covariance matrix \mathcal{K} is not positive semidefinite is due to the approximation and the simplifications of the model mentioned in Figure 1 in calculating the covariance values, that is, due to the preciseness of (4) and (5), compared to the true covariance values. In other words, errors in estimating covariance values may exist in the calculation. Those errors may result in a covariance matrix being not positive semidefinite.

A question that could be raised here is why the covariance matrix of *complex Gaussian random variables* (with Rayleigh fading envelopes), rather than the covariance matrix of *Rayleigh envelopes*, is of particular interest. This is due to the two following reasons.

From the physical point of view, in the covariance matrix of *Rayleigh envelopes*, the correlation properties R_{xx} , R_{yy} of the real components (inphase components) as well as the imaginary components (quadrature phase components) themselves and the correlation properties R_{xy} , R_{yx} between the real and imaginary components of random variables are *not* directly present (these correlation properties are defined in (2)). On the contrary, those correlation properties are *clearly* present in the covariance matrix of complex Gaussian random variables with the desired Rayleigh envelopes. In other words, the physical significance of the correlation properties of random variables is *not* present as detailed in the covariance matrix of *Rayleigh envelopes* as in the covariance matrix of complex Gaussian random variables with the desired Rayleigh envelopes.

Further, from the mathematical point of view, it is possible to have one-to-one mapping *from* the cross-correlation coefficients ρ_{gij} (between the i th and j th complex Gaussian random variables) *to* the cross-correlation coefficients ρ_{rij}

(between Rayleigh fading envelopes) as follows (see [9, (1.5-26)]):

$$\rho_{rij} = \frac{(1 + |\rho_{gij}|)E_{\text{int}}\left(2\sqrt{|\rho_{gij}|}/(1 + |\rho_{gij}|)\right) - \pi/2}{2 - \pi/2}, \quad (12)$$

where $E_{\text{int}}(\cdot)$ is the complete elliptic integral of the second kind. Some good approximations of this relationship between ρ_{rij} and ρ_{gij} are presented in the mapping [4, Table II], the look-up [8, Table I and Figure 1].

However, the reversed mapping, that is, the mapping *from* ρ_{rij} *to* ρ_{gij} , is *multivalent*. It means that, for a given ρ_{rij} , we have to somehow determine ρ_{gij} in order to generate Rayleigh fading envelopes and the possible values of ρ_{gij} may be significantly different from each other depending on how ρ_{gij} is determined from ρ_{rij} . It is noted that ρ_{rij} is always real, but ρ_{gij} may be complex.

For the two aforementioned reasons, the covariance matrix of complex Gaussian random variables (with Rayleigh envelopes), as opposed to the covariance matrix of Rayleigh envelopes, is of particular interest in this paper.

4.2. Forced positive semidefiniteness of the covariance matrix

First, we need to define the *coloring matrix* \mathcal{L} corresponding to a covariance matrix \mathcal{K} . The *coloring matrix* \mathcal{L} is defined to be the $N \times N$ matrix satisfying

$$\mathcal{L}\mathcal{L}^H = \mathcal{K}. \quad (13)$$

It is noted that the coloring matrix is *not* necessarily a lower triangular matrix. Particularly, to determine the coloring matrix \mathcal{L} corresponding to a covariance matrix \mathcal{K} , we can use *either* Cholesky decomposition [7] as mentioned in a number of papers, which have been reviewed in Section 2 of this paper, *or* eigen decomposition which is mentioned in the next section of this paper. The former yields a lower triangular coloring matrix, while the later yields a square coloring matrix.

Unlike Cholesky decomposition, where the covariance matrix \mathcal{K} must be *positive definite*, eigen decomposition requires that \mathcal{K} is at least *positive semidefinite*, that is, the eigenvalues of \mathcal{K} are either zeros or positive. We will explain later why the covariance matrix must be positive semidefinite even in the case where eigen decomposition is used to calculate the coloring matrix. The covariance matrix \mathcal{K} , in fact, may *not* be positive semidefinite, that is, \mathcal{K} may have negative eigenvalues, as the case mentioned in Example 1 of Section 4.1.

To overcome this obstacle, similarly to (but not exactly as) the method in [2], we approximate the given covariance matrix by a matrix that can be decomposed into $\mathbf{K} = \mathbf{L}\mathbf{L}^H$. While the method in [2] does this by replacing all negative and zero eigenvalues by a small, positive real number, we only replace the negative ones by zeros. This is possible, because we base our decomposition on an eigen analysis instead of a Cholesky decomposition as in [2], which can only be carried

out if all eigenvalues are positive. Our procedure is presented as follows.

Assuming that \mathcal{K} is the desired covariance matrix, which is *not* positive semidefinite, perform the *eigen decomposition* $\mathcal{K} = \mathbf{V}\mathbf{G}\mathbf{V}^H$, where \mathbf{V} is the matrix of eigenvectors and \mathbf{G} is a diagonal matrix of eigenvalues of the matrix \mathcal{K} . Let $\mathbf{G} = \text{diag}(\lambda_1, \dots, \lambda_N)$. Calculate the approximate matrix $\mathbf{\Lambda} \triangleq \text{diag}(\hat{\lambda}_1, \dots, \hat{\lambda}_N)$, where

$$\hat{\lambda}_j = \begin{cases} \lambda_j & \text{if } \lambda_j \geq 0, \\ 0 & \text{if } \lambda_j < 0. \end{cases} \quad (14)$$

We now compare our approximation procedure to the approximation procedure mentioned in [2]. The authors in [2] used the following approximation:

$$\hat{\lambda}_j = \begin{cases} \lambda_j & \text{if } \lambda_j > 0, \\ \varepsilon & \text{if } \lambda_j \leq 0, \end{cases} \quad (15)$$

where ε is a small, positive real number.

Clearly, besides overcoming the disadvantage of Cholesky decomposition, our approximation procedure is *more precise* under realistic assumptions like finite precision arithmetic than the one mentioned in [2], since the matrix $\mathbf{\Lambda}$ in our algorithm approximates to the matrix \mathbf{G} better than the one mentioned in [2]. Therefore, the desired covariance matrix \mathcal{K} is well approximated by the positive semidefinite matrix $\mathbf{K} = \mathbf{V}\mathbf{\Lambda}\mathbf{V}^H$ from Frobenius point of view [2].

4.3. Determine the coloring matrix using eigen decomposition

In most of the conventional methods, Cholesky decomposition was used to determine the coloring matrix. As analyzed earlier in Section 2, Cholesky decomposition may not work for the covariance matrix which has eigenvalues being equal or close to zeros.

To overcome this disadvantage, we use eigen decomposition, instead of Cholesky decomposition, to calculate the coloring matrix. Comparison of the computational efforts between the two methods (eigen decomposition versus Cholesky decomposition) is mentioned later in this paper. The coloring matrix is calculated as follows.

At this stage, we have the forced positive semidefinite covariance matrix \mathbf{K} , which is equal to the desired covariance matrix \mathcal{K} if \mathcal{K} is positive semidefinite, or approximates to \mathcal{K} otherwise. Further, as mentioned earlier, we have $\mathbf{K} = \mathbf{V}\mathbf{\Lambda}\mathbf{V}^H$, where $\mathbf{\Lambda} = \text{diag}(\hat{\lambda}_1, \dots, \hat{\lambda}_N)$ is the matrix of eigenvalues of \mathbf{K} . Since \mathbf{K} is a positive semidefinite matrix, it follows that $\{\hat{\lambda}_j\}_{j=1}^N$ are *real* and *nonnegative*.

We now calculate a new matrix $\bar{\mathbf{\Lambda}}$ as

$$\bar{\mathbf{\Lambda}} = \sqrt{\mathbf{\Lambda}} = \text{diag} \left(\sqrt{\hat{\lambda}_1}, \dots, \sqrt{\hat{\lambda}_N} \right). \quad (16)$$

Clearly, $\bar{\mathbf{\Lambda}}$ is a *real, diagonal* matrix that results in

$$\bar{\mathbf{\Lambda}}\bar{\mathbf{\Lambda}}^H = \bar{\mathbf{\Lambda}}\bar{\mathbf{\Lambda}} = \mathbf{\Lambda}. \quad (17)$$

If we denote $\mathbf{L} \triangleq \mathbf{V}\bar{\mathbf{\Lambda}}$, then it follows that

$$\mathbf{L}\mathbf{L}^H = (\mathbf{V}\bar{\mathbf{\Lambda}})(\mathbf{V}\bar{\mathbf{\Lambda}})^H = \mathbf{V}\bar{\mathbf{\Lambda}}\bar{\mathbf{\Lambda}}^H\mathbf{V}^H = \mathbf{V}\mathbf{\Lambda}\mathbf{V}^H = \mathbf{K}. \quad (18)$$

It means that the coloring matrix \mathbf{L} corresponding to the covariance matrix \mathbf{K} can be computed *without* using Cholesky decomposition. Thereby, the shortcoming of [2], which is related to roundoff errors in Matlab caused by Cholesky decomposition and is pointed out in Section 2, can be overcome.

We now explain why the covariance matrix must be positive semidefinite even when eigen decomposition is used to compute the coloring matrix. It is easy to realize that, if \mathbf{K} is *not* positive semidefinite covariance matrix, then $\bar{\mathbf{\Lambda}}$ calculated by (16) is a *complex* matrix. As a result, (17) and (18) are not satisfied.

4.4. Proposed algorithm

In Section 2, we have shown that the method proposed in [2] fails to generate Rayleigh fading envelopes corresponding to a desired covariance matrix in a real-time scenario where Doppler frequency shifts are considered. This is because the authors in [2] did not realize the variance-changing effect caused by Doppler filters.

To surmount this shortcoming, the two following *simple, but important* modifications must be carried out.

- (1) Unlike step 6 of the method in [2], where N independent, complex Gaussian random variables (with Rayleigh fading envelopes) are generated with *unit* variances, in our algorithm, this step is modified in order to be able to generate independent, complex Gaussian random variables with *arbitrary* variances σ_g^2 . Correspondingly, step 7 of the method in [2] must also be modified. Besides being more generalized, the modification of our algorithm in steps 6 and 7 allows us to combine correctly the outputs of Doppler filters in the method proposed in [10] and our algorithm.
- (2) The variance-changing effect of Doppler filters must be considered. It means that, we have to calculate the variance of the outputs of Doppler filters, which may have an *arbitrary* value depending on the variance of the complex Gaussian random variables at the inputs of Doppler filters as well as the characteristics of those filters. The variance value of the outputs is then input into the step 6 which has been modified as mentioned above.

The modification (1) can be carried out in the algorithm generating Rayleigh fading envelopes in a *discrete-time* scenario (see the algorithm mentioned in this section). The modification (2) can be carried out in the algorithm generating Rayleigh fading envelopes in a real-time scenario *where*

Doppler frequency shifts are considered (see the algorithm mentioned in Section 5).

From the above observations, we propose here a generalized algorithm to generate N correlated Rayleigh envelopes in a single time instant as given below.

- (1) In a general case, the desired variances (powers) $\{\sigma_{g_j}^2\}_{j=1}^N$ of complex Gaussian random variables with Rayleigh envelopes must be known. Specially, if one wants to generate Rayleigh envelopes corresponding to the desired variances (powers) $\{\sigma_{r_j}^2\}_{j=1}^N$, then $\{\sigma_{g_j}^2\}_{j=1}^N$ are calculated as follows:³

$$\sigma_{g_j}^2 = \frac{\sigma_{r_j}^2}{(1 - \pi/4)} \quad \forall j = 1, \dots, N. \quad (19)$$

- (2) From the desired correlation properties of correlated complex Gaussian random variables with Rayleigh envelopes, determine the covariances $R_{xxk,j}$, $R_{yyk,j}$, $R_{xyk,j}$ and $R_{yxk,j}$, for $k, j = 1, \dots, N$ and $k \neq j$. In other words, in a general case, those covariances must be known. Specially, in the case where the powers of all random processes are *equal* and other conditions hold as mentioned in Sections 3.1 and 3.2, we can follow (3) in the case of time delay and frequency separation, such as in OFDM systems, or (4), (5), and (6) in the case of spatial separation like with multiple antennas in MIMO systems to calculate the covariances $R_{xxk,j}$, $R_{yyk,j}$, $R_{xyk,j}$, and $R_{yxk,j}$. The values $\{\sigma_{g_j}^2\}_{j=1}^N$, $R_{xxk,j}$, $R_{yyk,j}$, $R_{xyk,j}$, and $R_{yxk,j}$ ($k, j = 1, \dots, N$; $k \neq j$) are the input data of our proposed algorithm.
- (3) Create the $N \times N$ -sized covariance matrix \mathcal{K} :

$$\mathcal{K} = [\mu_{k,j}]_{N \times N}, \quad (20)$$

where

$$\mu_{k,j} = \begin{cases} \sigma_{g_j}^2 & \text{if } k \equiv j, \\ \begin{pmatrix} R_{xxk,j} + R_{yyk,j} \\ -i(R_{xyk,j} - R_{yxk,j}) \end{pmatrix} & \text{if } k \neq j. \end{cases} \quad (21)$$

The covariance matrix of complex Gaussian random variables is considered here, as opposed to the covariance matrix of Rayleigh fading envelopes like in the conventional methods.

- (4) Perform the eigen decomposition:

$$\mathcal{K} = \mathbf{V}\mathbf{G}\mathbf{V}^H. \quad (22)$$

Denote $\mathbf{G} \triangleq \text{diag}(\lambda_1, \dots, \lambda_N)$. Then, calculate a new

diagonal matrix:

$$\mathbf{\Lambda} = \text{diag}(\hat{\lambda}_1, \dots, \hat{\lambda}_N), \quad (23)$$

where

$$\hat{\lambda}_j = \begin{cases} \lambda_j & \text{if } \lambda_j \geq 0, \\ 0 & \text{if } \lambda_j < 0, \end{cases} \quad j = 1, \dots, N. \quad (24)$$

Thereby, we have a diagonal matrix $\mathbf{\Lambda}$ with all elements in the main diagonal being *real* and definitely *nonnegative*.

- (5) Determine a new matrix $\bar{\mathbf{\Lambda}} = \sqrt{\mathbf{\Lambda}}$ and calculate the coloring matrix \mathbf{L} by setting $\mathbf{L} = \mathbf{V}\bar{\mathbf{\Lambda}}$.
- (6) Generate a column vector \mathbb{W} of N *independent* complex Gaussian random samples with zero means and *arbitrary, equal* variances σ_g^2 :

$$\mathbb{W} = (u_1, \dots, u_N)^T. \quad (25)$$

We can see that the modification (1) takes place in this step of our algorithm and proceeds in the next step.

- (7) Generate a column vector \mathbb{Z} of N *correlated* complex Gaussian random samples as follows:

$$\mathbb{Z} = \frac{\mathbf{L}\mathbb{W}}{\sigma_g} \triangleq (z_1, \dots, z_N)^T. \quad (26)$$

As shown later in the next section, the elements $\{z_j\}_{j=1}^N$ are zero-mean, (*correlated*) complex Gaussian random variables with variances $\{\sigma_{g_j}^2\}_{j=1}^N$. The N moduli $\{r_j\}_{j=1}^N$ of the Gaussian samples in \mathbb{Z} are the *desired* Rayleigh fading envelopes.

4.5. Statistical properties of the resultant envelopes

In this section, we check the covariance matrix and the variances (powers) of the resultant correlated complex Gaussian random samples as well as the variances (powers) of the resultant Rayleigh fading envelopes.

It is easy to check that $E(\mathbb{W}\mathbb{W}^H) = \sigma_g^2 \mathbf{I}_N$, and therefore

$$E(\mathbb{Z}\mathbb{Z}^H) = E\left(\frac{\mathbf{L}\mathbb{W}\mathbb{W}^H\mathbf{L}^H}{\sigma_g^2}\right) = E(\mathbf{L}\mathbf{L}^H) = \mathbf{K}. \quad (27)$$

It means that the generated Rayleigh envelopes are corresponding to the forced positive semidefinite covariance matrix \mathbf{K} , which is, in turn, *equal* to the desired covariance matrix \mathcal{K} in case \mathcal{K} is *positive semidefinite*, or *well approximates* to \mathcal{K} otherwise. In other words, the desired covariance matrix \mathcal{K} of complex Gaussian random variables (with Rayleigh fading envelopes) is achieved.

In addition, note that the variance of the j th Gaussian random variable in \mathbb{Z} is the j th element on the main diagonal of \mathbf{K} . Because \mathbf{K} approximates to \mathcal{K} , the elements on the

³Note that $\sigma_{g_j}^2$ is the variance of *complex* Gaussian random variables, rather than the variance per dimension (real or imaginary). Hence, there is no factor of 2 in the denominator.

main diagonal of \mathbf{K} are thus equal (or close) to $\sigma_{g_j}^2$'s (see (20) and (21)). As a result, the resultant complex Gaussian random variables $\{z_j\}_{j=1}^N$ in \mathbb{Z} have zero means and variances (powers) $\{\sigma_{g_j}^2\}_{j=1}^N$.

It is known that the means and the variances of Rayleigh envelopes $\{r_j\}_{j=1}^N$ have the relation with the variances of the corresponding complex Gaussian random variables $\{z_j\}_{j=1}^N$ in \mathbb{Z} as given below (see [11, (5.51) and (5.52)] and [12, (2.1-131)]):

$$\begin{aligned} E\{r_j\} &= \sigma_{g_j} \frac{\sqrt{\pi}}{2} = 0.8862\sigma_{g_j}, \\ \text{Var}\{r_j\} &= \sigma_{g_j}^2 \left(1 - \frac{\pi}{4}\right) = 0.2146\sigma_{g_j}^2. \end{aligned} \quad (28)$$

From (19) and (28), it is clear that

$$\begin{aligned} E\{r_j\} &= \sigma_{r_j} \sqrt{\frac{\pi}{4 - \pi}}, \\ \text{Var}\{r_j\} &= \sigma_{r_j}^2. \end{aligned} \quad (29)$$

Therefore, the *desired* variances (powers) $\{\sigma_{r_j}^2\}_{j=1}^N$ of Rayleigh envelopes are achieved.

5. GENERATION OF CORRELATED RAYLEIGH ENVELOPES IN A REAL-TIME SCENARIO

In Section 4.4, we have proposed the algorithm for generating N correlated Rayleigh fading envelopes in multipath, flat fading channels in a *single time instant*. We can repeat steps 6 and 7 of this algorithm to generate Rayleigh envelopes in the *continuous time interval*. It is noted that, the discrete-time samples of each Rayleigh fading process generated by this algorithm in *different* time instants are *independent* of each other.

It has been known that the discrete-time samples of each *realistic* Rayleigh fading process may have *autocorrelation* properties, which are the functions of the Doppler frequency corresponding to the motion of receivers as well as other factors such as the sampling frequency of transmitted signals. It is because the band-limited communication channels not only limit the bandwidth of transmitted signals, but also limit the bandwidth of fading. This filtering effect limits the rate of changes of fading in time domain, and consequently, results in the autocorrelation properties of fading. Therefore, the algorithm generating Rayleigh fading envelopes in *realistic* conditions must consider the autocorrelation properties of Rayleigh fading envelopes.

To simulate a multipath fading channel, Doppler filters are normally used [11]. The analysis of Doppler spectrum spread was first derived by Gans [13], based on Clarke's model [14]. Motivated by these works, Smith [15] developed a computer-assisted model generating an *individual* Rayleigh fading envelope in flat fading channels corresponding to a given *normalized autocorrelation* function. This model was

then modified by Young [10, 16] to provide more accurate channel realization.

It should be emphasized that, in [10, 16], the models are aimed at generating an *individual* Rayleigh envelope corresponding to a certain normalized *autocorrelation* function of itself, rather than generating different Rayleigh envelopes corresponding to a desired covariance matrix (*autocorrelation* and *cross-correlation* properties between those envelopes).

Therefore, the model for generating N correlated Rayleigh fading envelopes in realistic fading channels (each individual envelope is corresponding to a desired normalized autocorrelation property) can be created by associating the model proposed in [10] with our algorithm mentioned in Section 4.4 in such a way that, the resultant Rayleigh fading envelopes are corresponding to the desired covariance matrix.

This combination must overcome the main shortcoming of the method proposed in [2] as analyzed in Section 2. In other words, the modification (2) mentioned in Section 4.4 must be carried out. This is an easy task in our algorithm. The key for the success of this task is the modification in steps 6 and 7 of our algorithm (see Section 4.4), where the variances of N complex Gaussian random variables are *not fixed* as in [2], but can be *arbitrary* in our algorithm. Again, besides being more generalized, our modification in these steps allows the *accurate* combination of the method proposed in [10] and our algorithm, that is, guaranteeing that the generated Rayleigh envelopes are exactly corresponding to the desired covariance matrix.

The model of a Rayleigh fading generator for generating an *individual* baseband Rayleigh fading envelope proposed in [10, 16] is shown in Figure 2. This model generates a Rayleigh fading envelope using inverse discrete Fourier transform (IDFT), based on *independent* zero-mean Gaussian random variables weighted by appropriate Doppler filter coefficients. The sequence $\{u_j[l]\}_{l=0}^{M-1}$ of the complex Gaussian random samples at the output of the j th Rayleigh generator (Figure 2) can be expressed as

$$u_j[l] = \frac{1}{M} \sum_{k=0}^{M-1} U_j[k] e^{i(2\pi kl/M)}, \quad (30)$$

where

- (i) M denotes the number of points with which the IDFT is carried out;
- (ii) l is the discrete-time sample index ($l = 0, \dots, M - 1$);
- (iii) $U_j[k] = F[k]A_j[k] - iF[k]B_j[k]$;
- (iv) $\{F[k]\}$ are the Doppler filter coefficients.

For brevity, we omit the subscript j in the expressions, except when this subscript is necessary to emphasize. If we denote $u[l] = u_R[l] + iu_I[l]$, then it has been proved that, the *autocorrelation* property between the real parts $u_R[l]$ and $u_R[m]$ as well as that between the imaginary parts $u_I[l]$ and

$u_I[m]$ at different discrete-time instants l and m is as given below (see [10, (7)]):

$$\begin{aligned} r_{RR}[l, m] &= r_{II}[l, m] = r_{RR}[d] = r_{II}[d] \\ &= E\{u_R[l]u_R[m]\} = \frac{\sigma_{\text{orig}}^2}{M} \text{Re}\{g[d]\}, \end{aligned} \quad (31)$$

where $d \triangleq l - m$ is the sample lag, σ_{orig}^2 is the variance of the real, independent zero-mean Gaussian random sequences $\{A[k]\}$ and $\{B[k]\}$ at the inputs of Doppler filters, and the sequence $\{g[d]\}$ is the IDFT of $\{F[k]^2\}$, that is,

$$g[d] = \frac{1}{M} \sum_{k=0}^{M-1} F[k]^2 e^{i(2\pi kd/M)}. \quad (32)$$

Similarly, the correlation property between the real part $u_R[l]$ and the imaginary part $u_I[m]$ is calculated as (see [10, (8)])

$$r_{RI}[d] = E\{u_R[l]u_I[m]\} = \frac{\sigma_{\text{orig}}^2}{M} \text{Im}\{g[d]\}. \quad (33)$$

The mean value of the output sequence $\{u[l]\}$ has been proved to be zero (see [10, Appendix A]).

If $d = 0$ and $\{F[k]\}$ are real, from (31), (32) and (33), we have

$$F[k] = \begin{cases} 0, & k = 0, \\ \sqrt{\frac{1}{2\sqrt{1 - (k/Mf_m)^2}}}, & k = 1, \dots, k_m - 1, \\ \sqrt{\frac{k_m}{2} \left[\frac{\pi}{2} - \arctan\left(\frac{k_m - 1}{\sqrt{2k_m - 1}}\right) \right]}, & k = k_m, \\ 0, & k = k_m + 1, \dots, M - k_m - 1, \\ \sqrt{\frac{k_m}{2} \left[\frac{\pi}{2} - \arctan\left(\frac{k_m - 1}{\sqrt{2k_m - 1}}\right) \right]}, & k = M - k_m, \\ \sqrt{\frac{1}{2\sqrt{1 - ((M - k)/Mf_m)^2}}}, & k = M - k_m + 1, \dots, M - 2, M - 1. \end{cases} \quad (37)$$

In (37), $k_m \triangleq \lfloor f_m M \rfloor$, where $\lfloor \cdot \rfloor$ indicates the biggest rounded integer being less or equal to the argument.

It has been proved in [10] that the (real) filter coefficients in (37) will produce a complex Gaussian sequence with the *normalized autocorrelation* function $J_0(2\pi f_m d)$, and with the *expected independence* between the real and imaginary parts of Gaussian samples, that is, the correlation property in (33) is zero. The zero-correlation property between the real and imaginary parts is necessary in order that the resultant envelopes are Rayleigh distributed.

$$r_{RR}[0] = r_{II}[0] = E\{u_R[l]u_R[l]\} = \frac{\sigma_{\text{orig}}^2}{M^2} \sum_{k=0}^{M-1} F[k]^2, \quad (34)$$

$$r_{RI}[0] = E\{u_R[l]u_I[l]\} = 0.$$

Therefore, by definition, the variance of the sequence $\{u[l]\}$ at the output of the Rayleigh generator is

$$\sigma_g^2 \triangleq E\{u[l]u[l]^*\} = 2E\{u_R[l]u_R[l]\} = \frac{2\sigma_{\text{orig}}^2}{M^2} \sum_{k=0}^{M-1} F[k]^2, \quad (35)$$

where $*$ denotes the complex conjugate operation.

Let r_{nor} be

$$r_{\text{nor}} = \frac{r_{RR}[d]}{\sigma_g^2} = \frac{r_{II}[d]}{\sigma_g^2}, \quad (36)$$

that is, let r_{nor} be the autocorrelation function in (31) *normalized* by the variance σ_g^2 in (35). r_{nor} is called the *normalized autocorrelation* function.

To achieve a desired *normalized autocorrelation* function $r_{\text{nor}} = J_0(2\pi f_m d)$, where f_m is the maximum Doppler frequency F_m normalized by the sampling frequency F_s of the transmitted signals (i.e., $f_m = F_m/F_s$), the Doppler filter $\{F[k]\}$ is determined in Young's model [10, 16] as follows (see [10, (21)]):

Let us consider the variance σ_g^2 of the resultant complex Gaussian sequence at the output of Figure 2. We consider an example where $M = 4096$, $f_m = 0.05$ and $\sigma_{\text{orig}}^2 = 1/2$ (σ_{orig}^2 is the variance per dimension). From (35) and (37), we have $\sigma_g^2 = 1.8965 \times 10^{-5}$. Clearly, passing complex Gaussian random variables with unit variances through Doppler filters reduces significantly the variances of those variables. In general, the variances of the complex Gaussian random variables at the output of the Rayleigh simulator presented in Figure 2 can be *arbitrary*, depending on M , σ_{orig}^2 , and $\{F[k]\}$, that is,

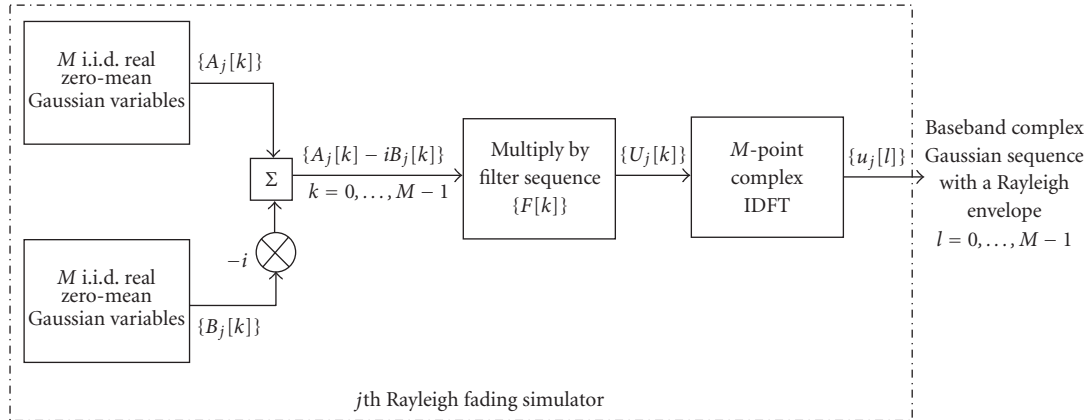


FIGURE 2: Model of a Rayleigh generator for an individual Rayleigh envelope corresponding to a desired *normalized* autocorrelation function.

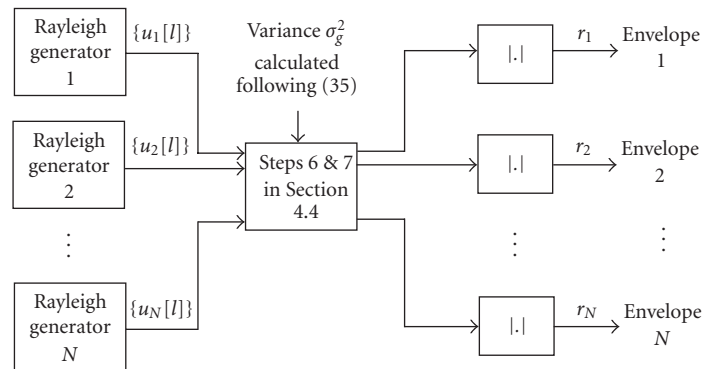


FIGURE 3: Model for generating N Rayleigh envelopes corresponding to a desired *normalized* autocorrelation function in a real-time scenario.

depending on the variances of the Gaussian random variables at the inputs of Doppler filters as well as the characteristics of those filters (see (35) for more details).

We now return to the main shortcoming of the method proposed in [2], which is mentioned earlier in Section 2. In [2, Section 6], the authors generated Rayleigh envelopes corresponding to a desired covariance matrix in a *real-time scenario*, where Doppler frequency shifts were considered, by combining their proposed method with the method proposed in [10]. Specifically, the authors took the outputs of the method in [10] and *simply* input them into step 6 in their method.

However, the step 6 in the method in [2] was proposed for generating complex Gaussian random variables with a *fixed* (unit) variance. Meanwhile, as presented earlier, the variances of the complex Gaussian random variables at the output of the Rayleigh simulator may have *arbitrary* values, depending on the variances of the Gaussian random variables at the inputs of Doppler filters as well as the characteristics of those filters. Consequently, if the outputs of the method in [10] are simply input into the step 6 as mentioned in the algorithm in [2], the covariance matrix of the resultant correlated Gaussian random variables is *not* equal to the de-

sired covariance matrix due to the variance-changing effect of Doppler filters being *not* considered. In other words, the method proposed in [2] *fails* to generate Rayleigh fading envelopes corresponding to a desired covariance matrix in a real-time scenario where Doppler frequency shifts are taken into account.

Our model for generating N correlated Rayleigh fading envelopes corresponding to a desired covariance matrix in a real-time scenario where Doppler frequency shifts are considered is presented in Figure 3. In this model, N Rayleigh generators, each of which is presented in Figure 2, are simultaneously used. To generate N *correlated* Rayleigh envelopes corresponding to a desired covariance matrix at an *observed discrete-time instant* l ($l = 0, \dots, M - 1$), similarly to the method in [2], we take the output $u_j[l]$ of the j th Rayleigh simulator, for $j = 1, \dots, N$, and input it as the element u_j into step 6 of our algorithm proposed in Section 4.4. However, as opposed to the method in [2], the variance σ_g^2 of complex Gaussian samples u_j in step 6 of our method is calculated following (35). This value is used as the input parameter for steps 6 and 7 of our algorithm (see Figure 3). Thereby, the variance-changing effect caused by Doppler filters is taken into consideration in our algorithm, and consequently, our

proposed algorithm overcomes the main shortcoming of the method in [2].

The algorithm for generating N correlated Rayleigh envelopes (when Doppler frequency shifts are considered) at a discrete-time instant l , for $l = 0, \dots, M - 1$, can be summarized as follows.

- (1) Perform the steps 1 to 5 mentioned in Section 4.4.
- (2) From the *desired autocorrelation* properties (31) and (36) of each of the complex Gaussian random sequences (with Rayleigh fading envelopes), determine the values M and σ_{orig}^2 . These values can be arbitrarily selected, provided that they bring about the desired autocorrelation properties. The value of M is also the number of points with which IDFT is carried out.
- (3) For each Rayleigh generator presented in Figure 2, generate M identically independently distributed (i.i.d.), *real*, zero-mean Gaussian random samples $\{A[k]\}$ with the variance σ_{orig}^2 and, independently, generate M i.i.d., *real*, zero-mean Gaussian samples $\{B[k]\}$ with the distribution $(0, \sigma_{\text{orig}}^2)$. From $\{A[k]\}$ and $\{B[k]\}$, generate M i.i.d. complex Gaussian random variables $\{A[k] - iB[k]\}$. N Rayleigh generators are simultaneously used to generate N Rayleigh envelopes as presented in Figure 3.
- (4) Multiply complex Gaussian samples $\{A[k] - iB[k]\}$, for $k = 1, \dots, M$, with the corresponding filter coefficient $F[k]$ given in (37).
- (5) Perform M -point IDFT of the resultant samples.
- (6) Calculate the variance σ_g^2 of the output $\{u[l]\}$ following (35). It is noted that σ_g^2 is the same for N Rayleigh generators. We also emphasize that, by this calculation, the modification (2) mentioned in Section 4.4 has been performed in this step.
- (7) Create a column vector $\mathbb{W} = (u_1, \dots, u_N)^T$ of N i.i.d. complex Gaussian random samples with the distribution $(0, \sigma_g^2)$ where the element u_j , for $j = 1, \dots, N$, is the output $u_j[l]$ of the j th Rayleigh generator and σ_g^2 has been calculated in step (6).
- (8) Continue the step 7 mentioned in Section 4.4. The N envelopes of elements in the column vector \mathbb{Z} are the desired Rayleigh envelopes at the considered time instant l .

Steps (7) and (8) are repeated for different time instants l ($l = 0, \dots, M - 1$), and therefore, the algorithm can be used for a real-time scenario.

6. SIMULATION RESULTS

In this section, first, we simulate $N = 3$ *frequency-correlated* Rayleigh fading envelopes corresponding to the complex Gaussian random variables with equal powers $\sigma_{g_j}^2 = 1$ ($j = 1, \dots, 3$) in the flat fading channels. Parameters considered here include $M = 2^{14}$ (the number of IDFT points), $\sigma_{\text{orig}}^2 = 1/2$ (variances per dimension in Young's model), $F_s = 8$ kHz, $F_m = 50$ Hz (corresponding to a carrier frequency 900 MHz and a mobile speed $v = 60$ km/h). Frequency

separation between two adjacent carrier frequencies considered here is $\Delta f = 200$ kHz (e.g., in GSM 900) and we assume that $f_1 > f_2 > f_3$. Also, we consider the rms delay spread $\sigma_\tau = 1$ microsecond and time delays between three envelopes are $\tau_{1,2} = 1$ millisecond, $\tau_{2,3} = 3$ milliseconds, $\tau_{1,3} = 4$ milliseconds.

From (3), (20), and (21), we have the *desired* covariance matrix \mathcal{K} as given below:

$$\mathcal{K} = \begin{bmatrix} 1 & 0.3782 + 0.4753i & 0.0878 + 0.2207i \\ 0.3782 - 0.4753i & 1 & 0.3063 + 0.3849i \\ 0.0878 - 0.2207i & 0.3063 - 0.3849i & 1 \end{bmatrix}. \quad (38)$$

It is easy to check that \mathcal{K} in (38) is positive definite. Using the proposed algorithm in Section 5, we have the simulation result presented in Figure 4a.

Next, we simulate $N = 3$ *spatially-correlated* Rayleigh fading envelopes. We consider an antenna array comprising three transmitter antennas, which are equally separated by a distance D . Assume that $D/\lambda = 1$, that is, $D = 33.3$ cm for GSM 900. Additionally, we assume that $\Delta = \pi/18$ rad (or $\Delta = 10^\circ$) and $\Phi = 0$ rad. The parameters M , $\sigma_{g_j}^2$, σ_{orig}^2 , F_s , and F_m are the same as in the previous case. From (4), (5), (6), (20), and (21), we have the following *desired* covariance matrix:

$$\mathcal{K} = \begin{bmatrix} 1 & 0.8123 & 0.3730 \\ 0.8123 & 1 & 0.8123 \\ 0.3730 & 0.8123 & 1 \end{bmatrix}. \quad (39)$$

Since $\Phi = 0$ rad, the covariances $R_{xyk,j}$ and $R_{yxk,j}$ between the real and imaginary components of any pair of the complex Gaussian random processes (with Rayleigh fading envelopes) are zeros, and consequently, \mathcal{K} is a *real* matrix. Readers may refer to (5) and (6) for more details. It is easy to realize that \mathcal{K} in (39) is positive definite. The simulation result is presented in Figure 4b.

In Figure 5a, we simulate $N = 3$ *frequency-correlated* Rayleigh envelopes based on IEEE 802.11a (OFDM) specifications [17]. In particular, the parameters considered here include $M = 2^{20}$, $\sigma_{g_j}^2 = 1$ ($j = 1, \dots, 3$), $\sigma_{\text{orig}}^2 = 1/2$, $F_s = 20$ MHz, $F_m = 555.56$ Hz (corresponding to a carrier frequency 5 GHz and a mobile speed $v = 120$ km/h), $\Delta f = 312.5$ kHz, $\sigma_\tau = 0.1$ microsecond, $\tau_{1,2} = \tau_{2,3} = 1$ millisecond, and $\tau_{1,3} = 2$ milliseconds. In Figure 5b, we simulate the case where the covariance matrix is not positive semidefinite as mentioned earlier in Example 1 of Section 4.1. From Figure 5b, we can realize that the three Rayleigh envelopes are highly correlated as we expect (see (11)).

In Figure 6, we plot the histograms of the resultant Rayleigh fading envelopes produced by our algorithm in the four aforementioned examples. Without loss of generality, we plot the histograms for one of three Rayleigh fading envelopes, such as the first Rayleigh fading envelope. To compare the accuracy of our algorithm, we also plot the *theoretical* probability density function (PDF) of a typical Rayleigh

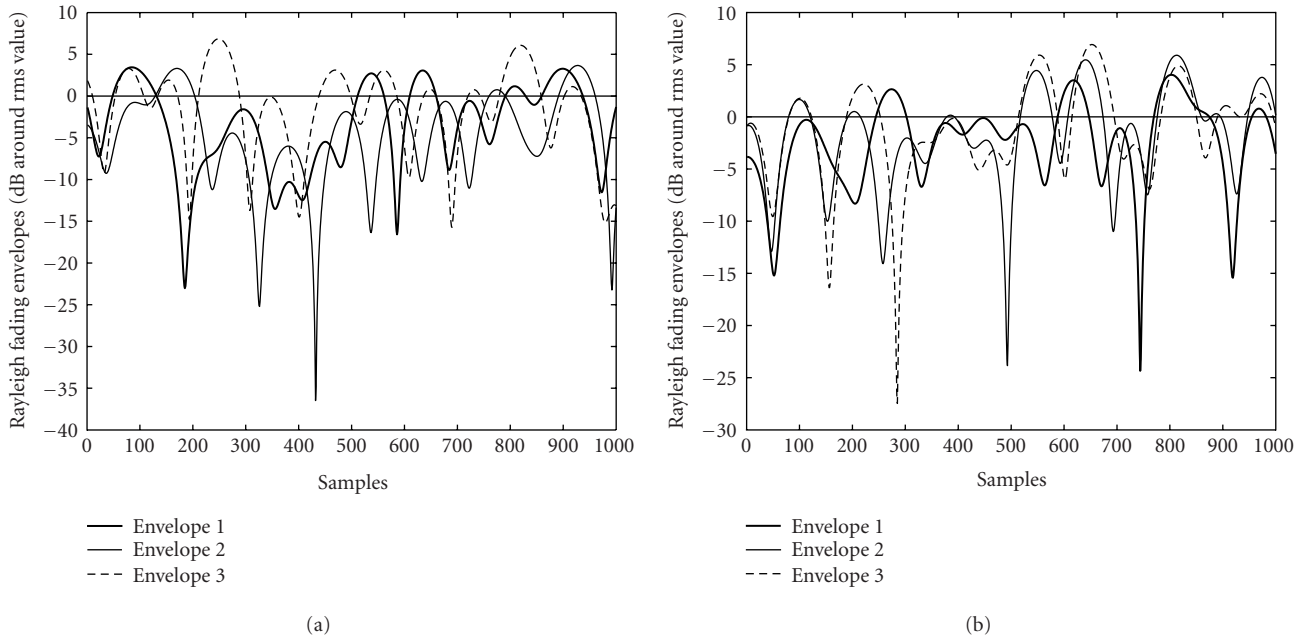


FIGURE 4: Examples of three equal power-correlated Rayleigh fading envelopes with GSM specifications. (a) Spectral correlation, GSM specifications. (b) Spatial correlation, GSM specifications.

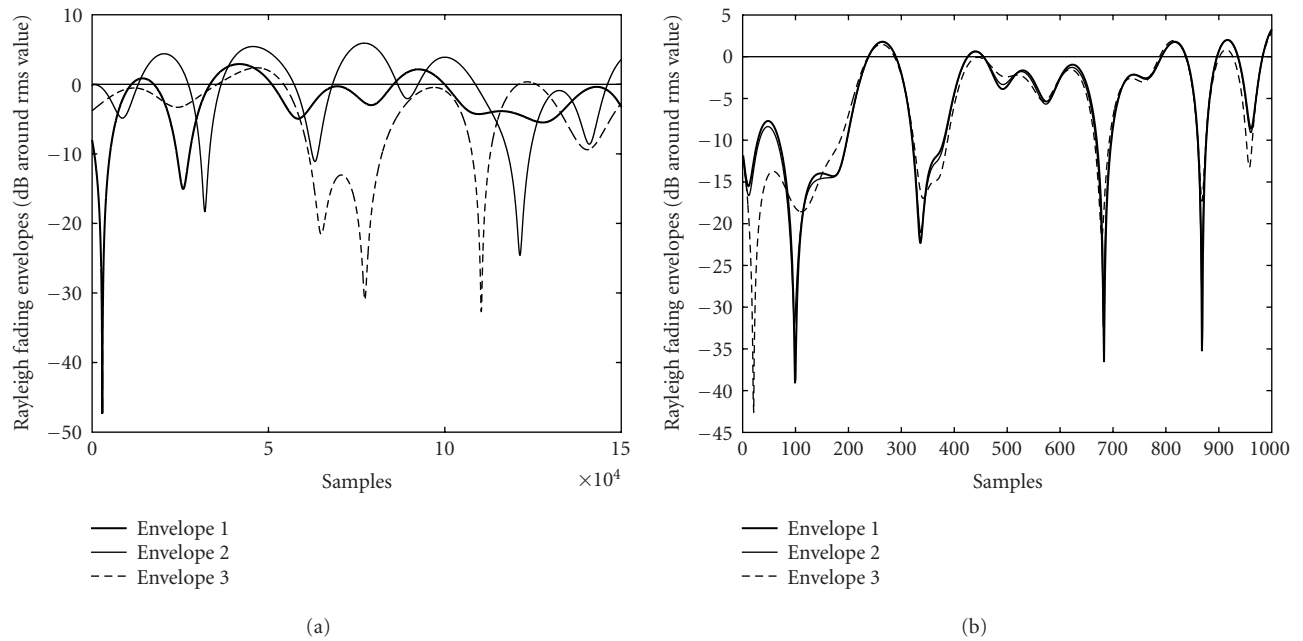


FIGURE 5: Examples of three equal power-correlated Rayleigh fading envelopes with IEEE 802.11a (OFDM) specifications, and with a not positive semidefinite covariance matrix. (a) Spectral correlation, OFDM specifications. (b) Spatial correlation, \mathcal{K} is not positive semidefinite.

fading envelope by solid curves. In this figure, the parameter $\sigma_{g_j}^2$ of the PDF is the variance of the *complex* Gaussian random process corresponding to the considered typical Rayleigh fading envelope. It can be observed from Figure 6 that, the resultant envelopes produced by our algorithm in

the four examples follow accurately the theoretical PDF of the typical Rayleigh fading envelope.

Finally, in Figure 7, we compare the computational efforts between our algorithm and the one mentioned in [2] by comparing the average computational time required for both

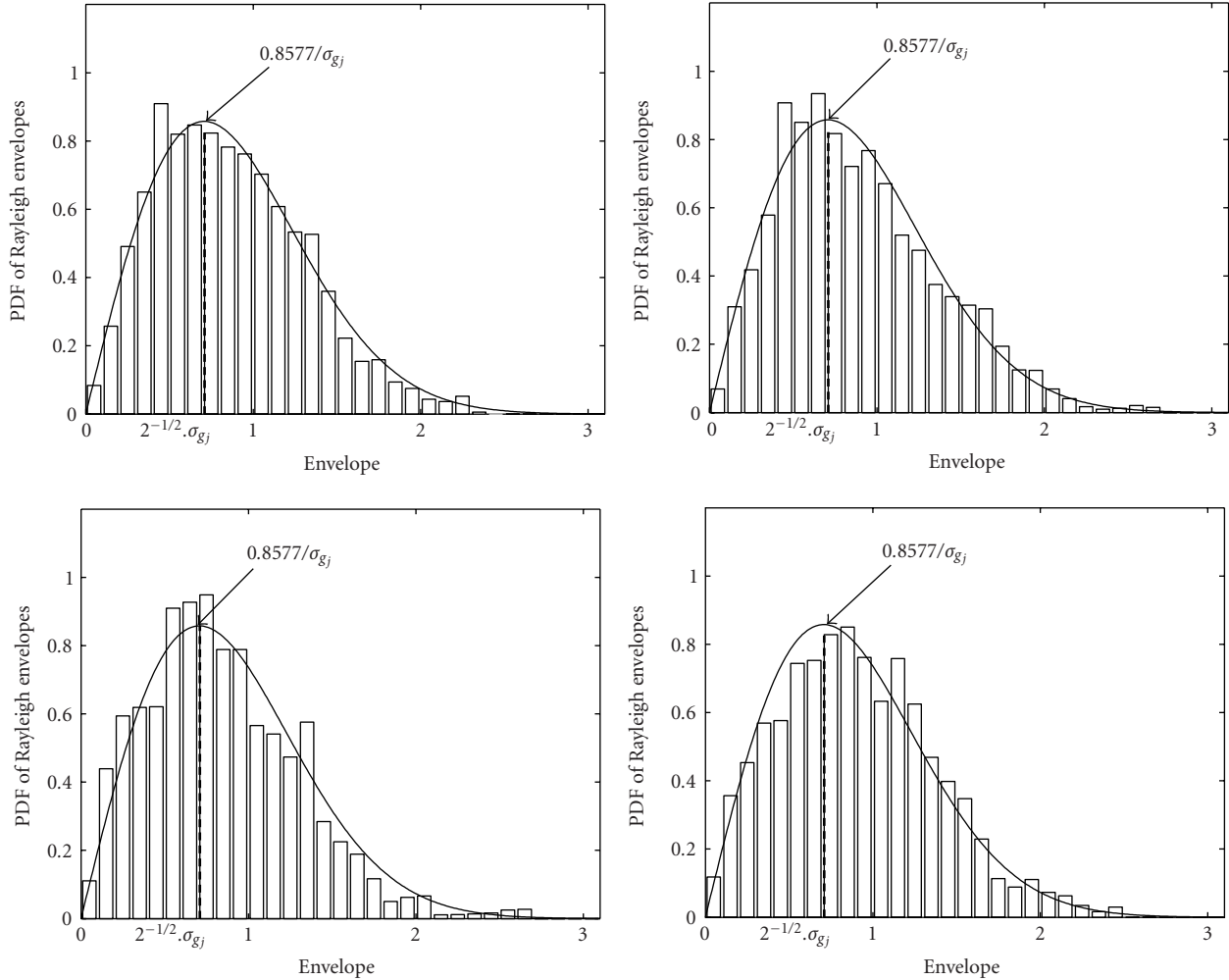


FIGURE 6: Histograms of Rayleigh fading envelopes produced by the proposed algorithm in the four examples along with a Rayleigh PDF where $\sigma_{g_j}^2 = 1$.

algorithms to simulate $N = 2, 4, 8, 16, 32, 64$ or 128 Rayleigh envelopes in a real-time scenario over 10 000 trials. It can be realized from Figure 7 that, for $N = 64$ and $N = 128$, our algorithm is slightly more complex, while it is almost as computationally efficient as the method in [2] for a smaller N .

7. CONCLUSIONS

In this paper, we have derived a more generalized algorithm to generate correlated Rayleigh fading envelopes. Using the presented algorithm, one can generate an arbitrary number N of either Rayleigh envelopes with any desired power $\sigma_{r_j}^2$, $j = 1, \dots, N$, or those envelopes corresponding to any desired power $\sigma_{g_j}^2$ of Gaussian random variables. This algorithm also facilitates to generate equal as well as unequal power Rayleigh envelopes. It is applicable to both scenarios of spatial correlation and spectral correlation between the random processes. The coloring matrix is determined by a positive semidefiniteness forcing procedure and an eigen decomposi-

tion procedure without using Cholesky decomposition. Consequently, the restriction on the positive definiteness of the covariance matrix is relaxed and the algorithm works well without being impeded by the roundoff errors of Matlab. The proposed algorithm can be used to generate Rayleigh envelopes corresponding to any desired covariance matrix, no matter whether or not it is positive definite. In comparison with the conventional methods, besides being more generalized, our proposed algorithm (with or without Doppler spectrum spread) is more precise, while overcoming all shortcomings of the conventional methods.

ACKNOWLEDGMENTS

The authors would like to thank the reviewers for the very helpful comments. Some results included in this paper were presented during the 5th IEEE International Workshop on Algorithms for Wireless, Mobile, Ad Hoc and Sensor Networks (IEEE WMAN 05), April 2005, and during the IEEE

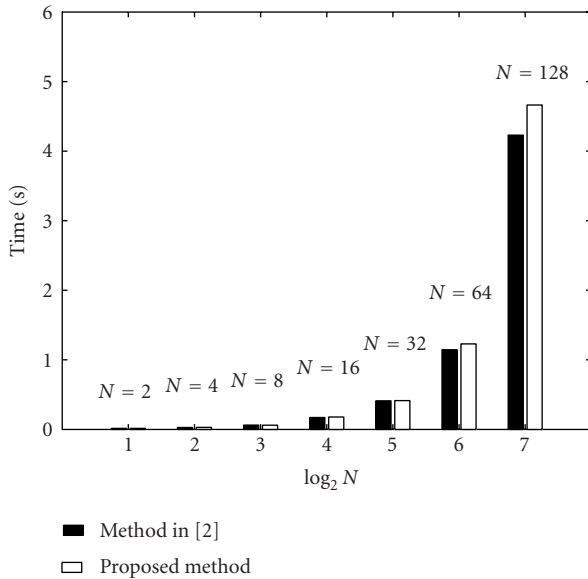


FIGURE 7: Computational effort comparison between the method in [2] and the proposed algorithm.

International Symposium on a World of Wireless, Mobile and Multimedia Networks (IEEE WOWMOM), June 2005.

REFERENCES

- [1] D. Verdin and T. C. Tozer, "Generating a fading process for the simulation of land-mobile radio communications," *Electronics Letters*, vol. 29, no. 23, pp. 2011–2012, 1993.
- [2] S. Sorooshyari and D. G. Daut, "Generation of correlated Rayleigh fading envelopes for accurate performance analysis of diversity systems," in *Proc. 14th IEEE International Symposium on Personal, Indoor and Mobile Radio Communications (PIMRC '03)*, vol. 2, pp. 1800–1804, Beijing, China, September 2003.
- [3] J. Salz and J. H. Winters, "Effect of fading correlation on adaptive arrays in digital mobile radio," *IEEE Trans. Veh. Technol.*, vol. 43, no. 4, pp. 1049–1057, 1994.
- [4] R. B. Ertel and J. H. Reed, "Generation of two equal power correlated Rayleigh fading envelopes," *IEEE Commun. Lett.*, vol. 2, no. 10, pp. 276–278, 1998.
- [5] N. C. Beaulieu, "Generation of correlated Rayleigh fading envelopes," *IEEE Commun. Lett.*, vol. 3, no. 6, pp. 172–174, 1999.
- [6] N. C. Beaulieu and M. L. Merani, "Efficient simulation of correlated diversity channels," in *Proc. IEEE Conference on Wireless Communications and Networking (WCNC '00)*, vol. 1, pp. 207–210, Chicago, Ill, USA, September 2000.
- [7] H. Adeli and R. Soegiarso, *High-Performance Computing in Structural Engineering*, CRC Press, Boca Raton, Fla, USA, 1999.
- [8] B. Natarajan, C. R. Nassar, and V. Chandrasekhar, "Generation of correlated Rayleigh fading envelopes for spread spectrum applications," *IEEE Commun. Lett.*, vol. 4, no. 1, pp. 9–11, 2000.
- [9] W. C. Jakes, *Microwave Mobile Communications*, John Wiley & Sons, New York, NY, USA, 1974.
- [10] D. J. Young and N. C. Beaulieu, "The generation of correlated Rayleigh random variates by inverse discrete Fourier transform," *IEEE Trans. Commun.*, vol. 48, no. 7, pp. 1114–1127, 2000.
- [11] T. S. Rappaport, *Wireless Communications: Principles and Practice*, Prentice Hall PTR, Upper Saddle River, NJ, USA, 2nd edition, 2002.
- [12] J. G. Proakis, *Digital Communications*, McGraw-Hill, Boston, Mass, USA, 4th edition, 2001.
- [13] M. J. Gans, "A power spectral theory of propagation in the mobile radio environment," *IEEE Trans. Veh. Technol.*, vol. VT-21, no. 1, pp. 27–38, 1972.
- [14] R. H. Clarke, "A statistical theory of mobile-radio reception," *Bell System Technical Journal*, vol. 47, no. 6, pp. 957–1000, 1968.
- [15] J. I. Smith, "A computer generated multipath fading simulation for mobile radio," *IEEE Trans. Veh. Technol.*, vol. VT-24, no. 3, pp. 39–40, 1975.
- [16] D. J. Young and N. C. Beaulieu, "On the generation of correlated Rayleigh random variates by inverse discrete Fourier transform," in *Proc. 5th IEEE International Conference on Universal Personal Communications (ICUPC '96)*, vol. 1, pp. 231–235, Cambridge, Mass, USA, September–October 1996.
- [17] IEEE Standards Association, "Part 11: Wireless LAN medium access control (MAC) and physical layer (PHY) specifications—High-speed physical layer in the 5 GHz band," 1999, IEEE Standards Association [Online]. available: <http://standards.ieee.org/getieee802/>.

Le Chung Tran received the excellent B. Eng. degree with the highest distinction and the M. Eng. degree with the highest distinction in telecommunications engineering from Hanoi University of Communications and Transport and Hanoi University of Technology, Vietnam, in 1997 and 2000, respectively. From March 2002 to July 2005, he worked towards the Ph.D. degree in telecommunications engineering at the School of Electrical, Computer and Telecommunications Engineering, University of Wollongong, Australia. He is currently working as an Associate Research Fellow at the Telecommunications and Information Technology Research Institute (TITR), School of Electrical, Computer and Telecommunications Engineering, University of Wollongong, Australia. He has been working as a Lecturer at Hanoi University of Communications and Transport, Vietnam, since September 1997 to date. He has achieved numerous national and overseas awards, including World University Services (WUS) (twice), Vietnamese Government's Scholarship, Wollongong University Postgraduate Award (UPA), Wollongong University Tuition Fee Waiver, during the undergraduate and postgraduate periods. His research interests include transmission diversity techniques, mobile communications, space-time processing, MIMO systems, channel propagation modelling, ultra-wideband communications, OFDM, and spread-spectrum techniques. He is a Member of IEEE.



Tadeusz A. Wysocki received the M.S.Eng. degree with the highest distinction in telecommunications from the Academy of Technology and Agriculture, Bydgoszcz, Poland, in 1981. In 1984, he received his Ph.D. degree, and in 1990, was awarded a D.S. degree (habilitation) in telecommunications from the Warsaw University of Technology. In 1992, he moved to Perth, Western Australia, to work at Edith Cowan University. He spent the whole of 1993 at the University of Hagen, Germany, within the framework of Alexander von Humboldt Research



Fellowship. After returning to Australia, he was appointed a Program Leader, Wireless Systems, within Cooperative Research Centre for Broadband Telecommunications and Networking. Since December 1998, he has been working as an Associate Professor at the University of Wollongong, NSW, within the School of Electrical, Computer and Telecommunications Engineering. The main areas of his research interests include indoor propagation of microwaves, code division multiple access (CDMA), and digital modulation and coding schemes. He is the author or coauthor of four books, over 100 research publications, and nine patents. He is a Senior Member of IEEE.

Alfred Mertins received his Dipl.-Ing. degree from the University of Paderborn, Germany, in 1984, the Dr.-Ing. degree in electrical engineering and the Dr.-Ing. Habil. degree in telecommunications from the Hamburg University of Technology, Germany, in 1991 and 1994, respectively. From 1986 to 1991 he was with the Hamburg University of Technology, Germany, from 1991 to 1995 with the Microelectronics Applications Center, Hamburg, Germany, from 1996 to 1997 with the University of Kiel, Germany, from 1997 to 1998 with the University of Western Australia, and from 1998 to 2003 with the University of Wollongong, Australia. In April 2003, he joined the University of Oldenburg, Germany, where he is a Professor in the Faculty of Mathematics and Science. His research interests include speech, audio, image and video processing, wavelets and filter banks, and digital communications. He is a Senior Member of IEEE.



Jennifer Seberry received the Ph.D. degree in computation mathematics from La Trobe University in 1971. She has subsequently held positions at the Australian National University, The University of Sydney and ADFA, The University of New South Wales. She has published extensively in discrete mathematics and is world renown for her new discoveries on Hadamard matrices and statistical designs. In 1970 she cofounded the series of conferences known as the xxth Australian Conference on Combinatorial Mathematics and Combinatorial Computing. She started teaching in cryptology and computer security in 1980. She is especially interested in authentication and privacy. In 1987, at University College, ADFA, she founded the Centre for Computer and Communications Security Research which proved to be a reservoir of expertise for the Australian community. Her studies of the application of discrete mathematics and combinatorial computing via bent functions, S-box design, has led to the design of secure cryptoalgorithms and strong hashing algorithms for secure and reliable information transfer in networks and telecommunications. Her studies of Hadamard matrices and orthogonal designs are applied in CDMA technologies. In 1990 she founded the AUSCRYPT/ASIACRYPT series of International Cryptologic Conferences in the Asia/Oceania area. She has supervised 25 successful Ph.D. candidates, has over 350 scholarly papers and six books. She is a Senior Member of IEEE.



Special Issue on Wireless Mobile Ad Hoc Networks

Call for Papers

Wireless mobile ad hoc networks (MANETs), due to their dynamic nature, pose many unique challenges compared to traditional wired or cellular wireless networks. MANETs must be self-organized without any requirement for base stations. Their topologies are unpredictable due to mobility and change with the number and distribution of active nodes in the network. Fading and channel variations also induce changes in the network topology and introduce additional complexities in these networks. Given power and energy constraints, as well as the shared nature of the wireless medium, communications may be expected to be multihop. In such a harsh environment, robustness and quality of service (QoS) are essential factors to be considered. MANETs may consist of a heterogeneous mixture of nodes with variety of traffic types and different QoS requirements. Scaling laws for these networks are not fully understood. Many tradeoff studies related to capacity, delay, bandwidth, and energy consumption are currently under intense investigations.

The goal of this special issue is to collect cutting-edge research results in the field of wireless MANETs. We solicit papers that deal with pressing problems unique to wireless MANETs. The scope of this issue includes all aspects of MANETs, including scaling laws, tradeoff studies, coding, interference management, protocol design, cross-layer design, and, more importantly, fundamental limits of MANETs under different conditions. We seek original and unpublished work. The potential list of topics is not necessarily exhaustive and other appropriate subjects will be considered.

Topics of interest include (but are not limited to):

- Analytical framework and appropriate metrics for evaluation of MANETs
- Fundamental limits of multihop MANETs
- Capacity, delay, bandwidth, and energy tradeoffs
- Scalable energy-efficient protocols, and framework for analysis of protocols
- Error control schemes
- Network coding
- Interference management
- Cross-layer design
- Cooperation among nodes

- Hybrid networks containing static and mobile nodes
- QoS support for different traffic types

Authors should follow the EURASIP JWCN manuscript format described at <http://www.hindawi.com/journals/wcn/>. Prospective authors should submit an electronic copy of their complete manuscript through the EURASIP JWCN manuscript tracking system at <http://www.mstracking.com/wcn/>, according to the following timetable:

Manuscript Due	February 1, 2006
Acceptance Notification	June 1, 2006
Final Manuscript Due	September 1, 2006
Publication Date	4rd Quarter, 2006

GUEST EDITORS:

Hamid R. Sadjadpour, Baskin School of Engineering, University of California, Santa Cruz, CA 95064, USA; hamid@soe.ucsc.edu

Robert Ulman, Army Research Office, Research Triangle Park, NC 27709, USA; robert.ulman@us.army.mil

Anthony Ephremides, Department of Electrical Engineering, University of Maryland at College Park, MD 20742, USA; etony@mintaka.isr.umd.edu

Ananthram Swami, Army Research Lab, Adelphi, MD 20783-1197, USA; aswami@arl.army.mil

Special Issue on Space-Time Channel Modeling for Wireless Communications

Call for Papers

Multiple-input multiple-output (MIMO) wireless communication systems exploit the spatial channel created by transmit and receive antenna arrays to increase quality, capacity, and coverage in wireless communication systems. A wide variety of techniques, including space-time coding, spatial multiplexing schemes, transmitter-receiver architecture, precoding methods together with established physical layer algorithms have been proposed or adopted for MIMO communication systems. Channel modeling plays an important part in validating and proving these systems. Despite rapid progress in MIMO communication systems, lack of understanding and modeling of spatial aspects of wireless channels is a critical obstacle to the further development of this technology.

Topics of interest include (but are not limited to):

- Space-time channel models based on physical propagation mechanisms
- MIMO channel simulators
- Channel models based on measurements
- Spatial correlation
- Fast fading and/or frequency-selective channels
- MIMO channel measurements
- Statistical MIMO channel models
- Modeling and measurement of angular power distributions
- Broadband MIMO channel models
- Spatial aspects of UWB and 60 GHz channels
- Multiuser MIMO channel models

Authors should follow the EURASIP JWCN manuscript format described at <http://www.hindawi.com/journals/wcn/>. Prospective authors should submit an electronic copy of their complete manuscript through the EURASIP JWCN's manuscript tracking system at <http://www.mstracking.com/wcn/>, according to the following timetable:

Manuscript Due	April 1, 2006
Acceptance Notification	August 1, 2006
Final Manuscript Due	November 1, 2006
Publication Date	1st Quarter, 2007

GUEST EDITORS:

Thushara Abhayapala, Research School of Information Sciences and Engineering, The Australian National University, Canberra, Australia;
thushara.abhayapala@anu.edu.au

Mérouane Debbah, Eurécom Institute, Sophia Antipolis, France; merouane.debbah@eurecom.fr

Rodney Kennedy, Wireless Signal Processing Program, National ICT Australia (NICTA), Australia;
rodney.kennedy@anu.edu.au

Special Issue on Millimeter-Wave Wireless Communication Systems: Theory and Application

Call for Papers

In 2001, the United States Federal Communications Commission (FCC) reserved 7 GHz of unlicensed spectrum between 57 to 64 GHz for the purpose of wireless communications. As a result, the millimeter-wave- (mmWave-) based technology has received increased attention in both academia and industry for very high-data-rate wireless personal area network (WPAN) applications such as high-speed internet access, streaming content download (e.g., HDTV, home theater, etc.), real-time streaming, and wireless data bus for cable replacement. In addition to the high-data-rate applications, energy propagation in the 60 GHz band has unique characteristics that give many other benefits such as excellent immunity to interference, high security, and frequency reuse. This has been proven when an industrial standard such as IEEE 802.15.3c has been introduced to develop alternative PHY for the existing 802.15.3 WPAN Standard based on mmWave technology.

The aim of this special issue is to present research in mmWave communication systems with emphasis on future applications in wireless communications.

Topics of interest include (but are not limited to):

- Radio propagation measurement and modeling
- Antenna design
- Transmission technologies (e.g., modulation and detection)
- Algorithm and signal processing
- Synchronization and channel estimation
- Multiple access
- Standardization and regulation issue (e.g., IEEE 802.15.43c)
- RF transceiver frontend and subsystems design
- System design, implementation, and performance
- Circuit/RFIC design (e.g., SiGe, BiCMOS, CMOS, etc.)
- Multiple-antenna system (e.g., mmWave-MIMO)
- Wireless network and related issues
- Applications

Authors should follow the EURASIP JWCN manuscript format described at <http://www.hindawi.com/journals/wcn/>. Prospective authors should submit an electronic copy of their complete manuscript through the EURASIP JWCN's manuscript tracking system at <http://www.mstracking.com/wcn/>, according to the following timetable:

Manuscript Due	May 1, 2006
Acceptance Notification	September 1, 2006
Final Manuscript Due	December 1, 2006
Publication Date	1st Quarter, 2007

GUEST EDITORS:

Chia-Chin Chong, DoCoMo USA Labs, 181 Metro Drive, Suite 300, San Jose, CA 95110, USA; cchong@docomolabs-usa.com

Hiroyo Ogawa, Yokosuka Radio Communications Research Center, National Institute of Information and Communications Technology (NICT Yokosuka), 3-4, Hikarinooka, Yokosuka-shi, Kanagawa 239-0847, Japan; hogawa@nict.go.jp

Peter F. M. Smulders, Eindhoven University of Technology, P.O. Box 513, 5600 MB Eindhoven, The Netherlands; p.f.m.smulders@tue.nl

Su-Khiong Yong, Communication Lab, Samsung Advanced Institute of Technology, P.O. Box 111, Suwon 440-600, Korea; su.khiong.yong@samsung.com

Special Issue on Signal Processing with High Complexity: Prototyping and Industrial Design

Call for Papers

Some modern applications require an extraordinary large amount of complexity in signal processing algorithms. For example, the 3rd generation of wireless cellular systems is expected to require 1000 times more complexity when compared to its 2nd generation predecessors, and future 3GPP standards will aim for even more number-crunching applications. Video and multimedia applications do not only drive the complexity to new peaks in wired and wireless systems but also in personal and home devices. Also in acoustics, modern hearing aids or algorithms for de-reverberation of rooms, blind source separation, and multichannel echo cancellation are complexity hungry. At the same time, the anticipated products also put on additional constraints like size and power consumption when mobile and thus battery powered. Furthermore, due to new developments in electroacoustic transducer design, it is possible to design very small and effective loudspeakers. Unfortunately, the linearity assumption does not hold any more for this kind of loudspeakers, leading to computationally demanding nonlinear cancellation and equalization algorithms.

Since standard design techniques would either consume too much time or do not result in solutions satisfying all constraints, more efficient development techniques are required to speed up this crucial phase. In general, such developments are rather expensive due to the required extraordinary high complexity. Thus, de-risking of a future product based on rapid prototyping is often an alternative approach. However, since prototyping would delay the development, it often makes only sense when it is well embedded in the product design process. Rapid prototyping has thus evolved by applying new design techniques more suitable to support a quick time to market requirement.

This special issue focuses on new development methods for applications with high complexity in signal processing and on showing the improved design obtained by such methods. Examples of such methods are virtual prototyping, HW/SW partitioning, automatic design flows, float to fix conversions, automatic testing and verification, and power aware designs.

Authors should follow the EURASIP JES manuscript format described at <http://www.hindawi.com/journals/es/>. Prospective authors should submit an electronic copy of their complete manuscripts through the EURASIP JES's manuscript tracking system at <http://www.mstracking.com/es/>, according to the following timetable:

Manuscript Due	December 1, 2005
Acceptance Notification	March 1, 2006
Final Manuscript Due	June 1, 2006
Publication Date	3rd Quarter, 2006

GUEST EDITORS:

Markus Rupp, TU Wien, Gusshausstr. 25/389, A-1040 Wien, Austria; mrupp@nt.tuwien.ac.at

Thomas Kaiser, University of Duisburg-Essen, 47057 Duisburg, Germany; thomas.kaiser@uni-duisburg.de

Gerhard Schmidt, Harman Becker / Temic-SDS, Germany; gerhard.schmidt@temic-sds.com

Jean-Francois Nezan, IETR/Image group Lab, France; jean-francois.nezan@insa-rennes.fr

Special Issue on Field-Programmable Gate Arrays in Embedded Systems

Call for Papers

Field-Programmable Gate Arrays (FPGAs) are increasingly used in embedded systems to achieve high performance in a compact area. FPGAs are particularly well suited to processing data straight from sensors in embedded systems. More importantly, the reconfigurable aspects of FPGAs give the circuits the versatility to change their functionality based on processing requirements for different phases of an application, and for deploying new functionality.

Modern FPGAs integrate many different resources on a single chip. Embedded processors (both hard and soft cores), multipliers, RAM blocks, and DSP units are all available along with reconfigurable logic. Applications can use these heterogeneous resources to integrate several different functions on a single piece of silicon. This makes FPGAs particularly well suited to embedded applications.

This special issue focuses on applications that clearly show the benefit of using FPGAs in embedded applications, as well as on design tools that enable such applications. Specific topics of interest include the use of reconfiguration in embedded applications, hardware/software codesign targeting FPGAs, power-aware FPGA design, design environments for FPGAs, system signalling and protocols used by FPGAs in embedded environments, and system-level design targeting modern FPGA's heterogeneous resources.

Papers on other applicable topics will also be considered. All papers should address FPGA-based systems that are appropriate for embedded applications. Papers on subjects outside of this scope (i.e., not suitable for embedded applications) will not be considered.

Authors should follow the EURASIP JES manuscript format described at <http://www.hindawi.com/journals/es/>. Prospective authors should submit an electronic copy of their complete manuscript through the EURASIP JES manuscript tracking system at <http://www.mstracking.com/es/>, according to the following timetable:

Manuscript Due	December 15, 2005
Acceptance Notification	May 1, 2006
Final Manuscript Due	August 1, 2006
Publication Date	4th Quarter, 2006

GUEST EDITORS:

Miriam Leeser, Northeastern University, USA;
mel@coe.neu.edu

Scott Hauck, University of Washington, USA;
hauck@ee.washington.edu

Russell Tessier, University of Massachusetts, Amherst, USA;
tessier@ecs.umass.edu

Special Issue on Formal Methods for GALS Design

Call for Papers

As chips grow in speed and complexity, global control of an entire chip using a single clock is becoming increasingly challenging. In the future, multicore and large-scale systems-on-chip (SoC) designs are therefore likely to be composed of several timing domains.

Global Asynchrony and Local Synchrony (GALS) is emerging as the paradigm of choice for SoC design with multiple timing domains. In GALS systems, each timing domain is locally clocked, and asynchronous communication schemes are used to glue all of the domains together. Thus, unlike purely asynchronous design, GALS design is able to make use of the significant industrial investment in synchronous design tools.

There is an urgent need for the development of sound models and formal methods for GALS systems. In synchronous designs, formal methods and design automation have played an enabling role in the continuing quest for chips with ever greater complexity. Due to the inherent subtleties of the asynchronous circuit design, formal methods are likely to be vital to the success of the GALS paradigm.

We invite original articles for a special issue of the journal to be published in 2006. Articles may cover every aspect related to formal modeling and formal methods for GALS systems and/or target any type of embedded applications and/or architectures combining synchronous and asynchronous notions of timing:

- Formal design and synthesis techniques for GALS systems
- Design and architectural transformations and equivalences
- Formal verification of GALS systems
- Formal methods for analysis of GALS systems
- Hardware compilation of GALS system
- Latency-insensitive synchronous systems
- Mixed synchronous-asynchronous systems
- Synchronous/asynchronous interaction at different levels
- Clocking, interconnect, and interface issues in deep-submicron design

- Modeling of interfaces between multiple timing domains
- System decomposition into GALS systems
- Formal aspects of system-on-chip (SoC) and network-on-chip (NoC) designs
- Motivating case studies, comparisons, and applications

Authors should follow the EURASIP JES manuscript format described at <http://www.hindawi.com/journals/es/>. Prospective authors should submit an electronic copy of their complete manuscript through the EURASIP JES manuscript tracking system at <http://www.mstracking.com/es/>, according to the following timetable:

Manuscript Due	December 15, 2005
Acceptance Notification	April 15, 2006
Final Manuscript Due	July 15, 2006
Publication Date	4th Quarter, 2006

GUEST EDITORS:

Alain Girault, Pop Art Project, INRIA Rhône-Alpes, 38334 Saint-Ismier Cedex, France; alain.girault@inrialpes.fr

S. Ramesh, Department of Computer Science and Engineering, Indian Institute of Technology, Bombay, Mumbai-400 076, India; ramesh@cse.iitb.ac.in

Sandeep Kumar Shukla, Electrical and Computer Engineering Department, Virginia Tech, Blacksburg, VA 24061, USA; sandeep@cs.albany.edu

Jean-Pierre Talpin, ESPRESSO, IRISA/INRIA Rennes, 35042 Rennes Cedex, France; jean-pierre.talpin@irisa.fr

Special Issue on Embedded Vision System

Call for Papers

Vision systems allow computers to understand images, and to take appropriate actions, often under hard real-time constraints.

Most vision systems need high computer performance. The decisive constraint to develop pattern recognition or monitoring systems was therefore to consider computer hardware with excellent key features to fulfill the high requirements. This causality has several disadvantages. The costs of the final products are high, the size of the hardware becomes voluminous, the electromagnetic capability is reduced, and the energy consumption is often a problem. Therefore, the pressure to realize vision systems on the base of Embedded Systems was and is still increasing dramatically. Meanwhile, the number of possible applications has exploded since several disadvantages of classic systems can be avoided. The history of mobile phones evolution is one of the best examples. It would not have been possible without Embedded Systems, and especially not in such an affordable way. However, it is not necessary to consider only the mass market where Embedded Vision Systems can improve the current situation dramatically. If many cameras are installed to watch a scene, one is able to define a virtual camera, which always shows the most important angle of a view. If a bank note should be checked under the conditions of high accuracy, high probability of error recognition, and high throughput, the realization is only feasible, if the computer is assisted by a network of special parallelized chips. Usually, the algorithms can be divided into three areas, the prestage, where data is compressed, the specialized computational phase, and the interpretation stage. With this setup, the bandwidth and the data throughput may be improved in an amazing way.

Many other ideas could be presented. The main issues are the parallelization of processes, as well as the communications between them, which are based on networked chip sets. The challenge for the research work is to find optimal structures concerning real-time problems, energy consumption, low-price solutions, and so forth. However, not all algorithms for vision systems are suitable to be implemented in Embedded Systems; better solutions have to be discovered. In this sense many tasks and problems in the research field have to be solved, and many application areas are concerned.

This special issue focuses on new results of research work in the field of Embedded Vision Systems. Several main keywords are:

- Innovative architectures for embedded vision systems
- Innovative sensor systems for embedded vision applications
- Architectural considerations in complex image-processing programs in an embedded environment
- FPGA designs for image processing applications
- DSP and FPGA: alternative and/or complement
- Networking for distributed embedded vision systems
- Performance bottlenecks/solutions for high-performance vision systems
- Smart camera systems
- Virtual camera systems
- Object tracking
- Automotive applications
- Traffic flow measurement systems
- Robot and machine vision
- Bioinspired vision systems
- Verification methods for mission-critical embedded computer vision systems

Authors should follow the EURASIP JES manuscript format described at <http://www.hindawi.com/journals/es/>. Prospective authors should submit an electronic copy of their complete manuscript through the EURASIP JES manuscript tracking system at <http://www.mstracking.com/es/>, according to the following timetable:

Manuscript Due	May 1, 2006
Acceptance Notification	September 1, 2006
Final Manuscript Due	December 1, 2006
Publication Date	1st Quarter, 2007



GUEST EDITORS:

Dietmar Dietrich, Vienna University of Technology,
Gusshausstrasse 25-27/E384, 1040 Vienna, Austria;
dietrich@ict.tuwien.ac.at

Heinrich Garn, ARC Seibersdorf research GmbH, 2444
Seibersdorf, Austria; heinrich.garn@arcs.ac.at

Udo Keschull, Universität Heidelberg, Im Neuenheimer
Feld 227, 69120 Heidelberg, Germany;
keschul@kip.uni-heidelberg.de

Christoph Grimm, Institute of Microelectronic Systems,
University of Hannover, Appelstrasse 4, 30167 Hannover,
Germany; grimm@ims.uni-hannover.de

Moshe Ben-Ezra, Real-Time Vision and Modeling
Department, Siemens Corporate Research, 755 College
Road East, 08540 Princeton NJ, USA;
moshe.ben-ezra@siemens.com

Special Issue on Synchronous Paradigm in Embedded Systems

Call for Papers

Synchronous languages were introduced in the 1980s for programming reactive systems. Such systems are characterized by their continuous reaction to their environment, at a speed determined by the latter. Reactive systems include embedded control software and hardware. Synchronous languages have recently seen a tremendous interest from leading companies developing automatic control software and hardware for critical applications. Industrial success stories have been achieved by Schneider Electric, Airbus, Dassault Aviation, Snecma, MBDA, Arm, ST Microelectronics, Texas Instruments, Freescale, Intel The key advantage outlined by these companies resides in the rigorous mathematical semantics provided by the synchronous approach that allows system designers to develop critical software and hardware in a faster and safer way.

Indeed, an important feature of synchronous paradigm is that the tools and environments supporting development of synchronous programs are based upon a formal mathematical model defined by the semantics of the languages. The compilation involves the construction of these formal models, and their analysis for static properties, their optimization, the synthesis of executable sequential implementations, and the automated distribution of programs. It can also build a model of the dynamical behaviors, in the form of a transition system, upon which is based the analysis of dynamical properties, for example, through model-checking-based verification, or discrete controller synthesis. Hence, synchronous programming is at the crossroads of many approaches in compilation, formal analysis and verification techniques, and software or hardware implementations generation.

We invite original papers for a special issue of the journal to be published in the first quarter of 2007. Papers may be submitted on all aspects of the synchronous paradigm for embedded systems, including theory and applications. Some sample topics are:

- Synchronous languages design and compiling
- Novel application and implementation of synchronous languages
- Applications of synchronous design methods to embedded systems (hardware or software)

- Formal modeling, formal verification, controller synthesis, and abstract interpretation with synchronous-based tools
- Combining synchrony and asynchrony for embedded system design and, in particular, globally asynchronous and locally synchronous systems
- The role of synchronous models of computations in heterogeneous modeling
- The use of synchronous modeling techniques in model-driven design environment
- Design of distributed control systems using the synchronous paradigm

Authors should follow the EURASIP JES manuscript format described at <http://www.hindawi.com/journals/es/>. Prospective authors should submit an electronic copy of their complete manuscripts through the EURASIP JES's manuscript tracking system at <http://www.mstracking.com/es/>, according to the following timetable:

Manuscript Due	June 1, 2006
Acceptance Notification	October 1, 2006
Final Manuscript Due	December 1, 2006
Publication Date	1st Quarter, 2007

GUEST EDITORS:

Alain Girault, INRIA, France; alain.girault@inrialpes.fr

S. Ramesh, IIT Bombay, India; ramesh@cse.iitb.ac.in

Jean-Pierre Talpin, IRISA, France;

jean-pierre.talpin@irisa.fr

Special Issue on Embedded Systems for Portable and Mobile Video Platforms

Call for Papers

Video coding systems have been assuming an increasingly important role in application areas other than the traditional video broadcast and storage scenarios. Several new applications have emerged focusing on personal communications (such as video-conferencing), wireless multimedia, remote video-surveillance, and emergency systems. As a result, a number of new video compression standards have emerged addressing the requirements of these kinds of applications in terms of image quality and bandwidth. For example, the ISO/MPEG and ITU standardization bodies have recently jointly established the new AVC/H.264 video coding standard.

In such a wide range of applications scenarios, there is the need to adapt the video processing in general, and in particular video coding/decoding, to the restrictions imposed by both the applications themselves and the terminal devices. This problem is even more important for portable and battery-supplied devices, in which low-power considerations are important limiting constraints. Examples of such application requirements are currently found in 3G mobile phones, CMOS cameras and tele-assistance technologies for elderly/disabled people.

Therefore, the development of new power-efficient encoding algorithms and architectures suitable for mobile and battery-supplied devices is fundamental to enabling the widespread deployment of multimedia applications on portable and mobile video platforms. This special issue is focused on the design and development of embedded systems for portable and mobile video platforms. Topics of interest cover all aspects of this type of embedded system, including, not only algorithms, architectures, and specific SoC design methods, but also more technological aspects related to wireless-channels, power-efficient optimizations and implementations, such as encoding strategies, data flow optimizations, special coprocessors, arithmetic units, and electronic circuits.

Papers suitable for publication in this special issue must describe high-quality, original, unpublished research.

Prospective authors are invited to submit manuscripts on topics including but not limited to:

- Power-efficient algorithms and architectures for motion estimation, discrete transforms (e.g., SA-DCT, WT), integer transforms, and entropy coding
- Architectural paradigms for portable multimedia systems
- Low-power techniques and circuits, memory, and data flow optimizations for video coding
- Adaptive algorithms and generic configurable architectures for exploiting intrinsic characteristics of image sequences and video devices
- Aspects specifically important for portable and mobile video platforms, such as video transcoding, video processing in the compressed domain, and error resilience (e.g., MDC)
- Ultra-low-power embedded systems for video processing and coding
- Heterogeneous architectures, multithreading, MP-SoC, NoC implementations
- Design space exploration tools, performance evaluation tools, coding efficiency and complexity analysis tools for video coding in embedded systems

Authors should follow the EURASIP JES manuscript format described at <http://www.hindawi.com/journals/es/>. Prospective authors should submit an electronic copy of their complete manuscript through the EURASIP JES manuscript tracking system at <http://www.mstracking.com/es/>, according to the following timetable:

Manuscript Due	June 1, 2006
Acceptance Notification	October 1, 2006
Final Manuscript Due	January 1, 2007
Publication Date	2nd Quarter, 2007



GUEST EDITORS:

Leonel Sousa, INESC-ID, IST, Universidade Técnica de Lisboa, 1000-029 Lisboa, Portugal; las@inesc-id.pt

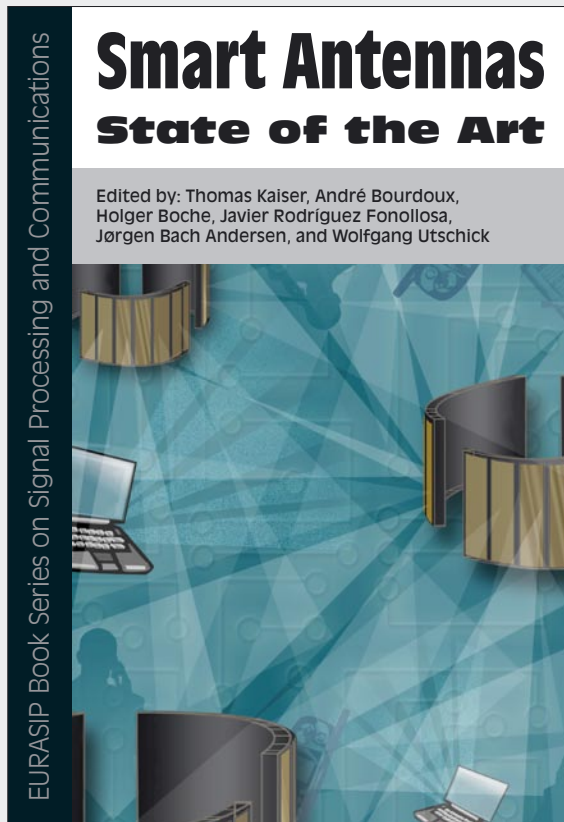
Noel O'Connor, School of Electronic Engineering, Dublin City University, Glasnevin, Dublin 9, Ireland; noel.oconnor@eeng.dcu.ie

Marco Mattavelli, Signal Processing Laboratory, Ecole Polytechnique Fédérale de Lausanne (EPFL), 1015 Lausanne, Switzerland; marco.mattavelli@epfl.ch

Antonio Nunez, IUMA, Universidad de Las Palmas de Gran Canaria, 35017 Las Palmas de Gran Canaria, Spain; nunez@iuma.ulpgc.es

SMART ANTENNAS—STATE OF THE ART

Edited by: Thomas Kaiser, André Bourdoux, Holger Boche, Javier Rodríguez Fonollosa, Jørgen Bach Andersen, and Wolfgang Utschick



Smart Antennas—State of the Art brings together the broad expertise of 41 European experts in smart antennas. They provide a comprehensive review and an extensive analysis of the recent progress and new results generated during the last years in almost all fields of smart antennas and MIMO (multiple input multiple output) transmission. The following represents a summarized table of content.

Receiver: space-time processing, antenna combining, reduced rank processing, robust beamforming, subspace methods, synchronization, equalization, multiuser detection, iterative methods

Channel: propagation, measurements and sounding, modeling, channel estimation, direction-of-arrival estimation, subscriber location estimation

Transmitter: space-time block coding, channel side information, unified design of linear transceivers, ill-conditioned channels, MIMO-MAC strategies

Network Theory: channel capacity, network capacity, multihop networks

Technology: antenna design, transceivers, demonstrators and testbeds, future air interfaces

Applications and Systems: 3G system and link level aspects, MIMO HSDPA, MIMO-WLAN/UMTS implementation issues

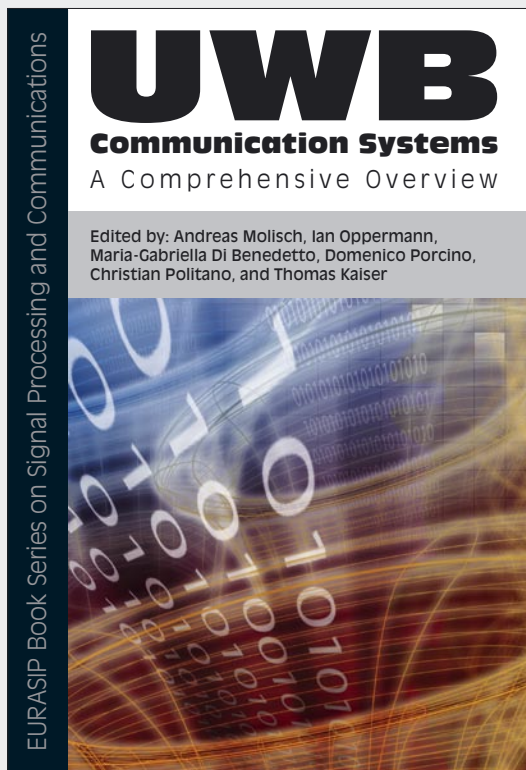
This book serves as a reference for scientists and engineers who need to be aware of the leading edge research in multiple-antenna communications, an essential technology for emerging broadband wireless systems.

For any inquiries on how to order this title please contact books.orders@hindawi.com

The EURASIP Book Series on Signal Processing and Communications publishes monographs, edited volumes, and textbooks on Signal Processing and Communications. For more information about the series please visit: <http://hindawi.com/books/spc/about.html>

UWB Communication Systems—A Comprehensive Overview

Edited by: Andreas Molisch, Ian Oppermann, Maria-Gabriella Di Benedetto, Domenico Porcino, Christian Politano, and Thomas Kaiser



Ultra-wideband (UWB) communication systems offer an unprecedented opportunity to impact the future communication world.

The enormous available bandwidth, the wide scope of the data rate/range trade-off, as well as the potential for very-low-cost operation leading to pervasive usage, all present a unique opportunity for UWB systems to impact the way people and intelligent machines communicate and interact with their environment.

The aim of this book is to provide an overview of the state of the art of UWB systems from theory to applications.

Due to the rapid progress of multidisciplinary UWB research, such an overview can only be achieved by combining the areas of expertise of several scientists in the field.

More than 30 leading UWB researchers and practitioners have contributed to this book covering the major topics relevant to UWB. These topics include UWB signal processing, UWB channel measurement and modeling, higher-layer protocol issues, spatial aspects of UWB signaling, UWB regulation and

standardization, implementation issues, and UWB applications as well as positioning.

The book is targeted at advanced academic researchers, wireless designers, and graduate students wishing to greatly enhance their knowledge of all aspects of UWB systems.

For any inquiries on how to order this title please contact books.orders@hindawi.com

The EURASIP Book Series on Signal Processing and Communications publishes monographs, edited volumes, and textbooks on Signal Processing and Communications. For more information about the series please visit: <http://hindawi.com/books/spc/about.html>